Assessment ~~and comparison~~ of thermal stabilisation measures based on numerical simulations at ~~an~~ a Swiss Alpine permafrost site~~, Switzerland~~

Elizaveta Sharaborova[1,2], Michael Lehning[1,2], Nander Wever[2], Marcia Phillips[2], and Hendrik Huwald[1,2]

[1]Environmental Engineering Institute, Laboratory of Cryospheric Sciences, Ecole Polytechnique Fédérale de Lausanne (EPFL) Valais/Wallis, Sion, Switzerland
[2]WSL Institute for Snow and Avalanche Research SLF, Davos, Switzerland

Correspondence: Elizaveta Sharaborova (elizaveta.sharaborova@epfl.ch)

Abstract. Global warming ~~provokes permafrost thawing , which leads~~ causes thawing of permafrost, leading to landscape changes and infrastructure damage, problems that have intensified worldwide in all permafrost regions. This study numerically investigates the impact of different thermal ~~stabilization methods to prevent or delay~~ stabilisation methods on preventing or delaying permafrost thawing. To test different technical methods, an alpine mountain permafrost site with nearby infrastructure ~~prone to damage~~ is investigated. Model simulations represent the one-dimensional effect of heat fluxes across the complex system of snow-ice-permafrost layers ~~,~~ and the impact of passive and active cooling, including engineered energy flux dynamics at the surface. ~~Results~~ The results show the efficiency of different passive, active ~~,~~ and combined thermal stabilisation methods ~~,~~ in influencing heat transfer, temperature distribution, and the seasonal active layer thickness. Investigating each component of thermal ~~stabilization~~ stabilisation helps quantify the efficiency of each method and determine their optimal combination. ~~Passive methods despite provide~~ Despite providing efficient cooling in winter, ~~due to heat transfer to the atmosphere,~~ passive methods are less efficient, as the active layer thickness remains over 1 m. Conductive heat flux ~~regulation~~ attenuation alone takes several years to form a stable frozen layer. Active cooling, when powered ~~with~~ by solar energy, ~~cooling~~ decreases the active layer thickness to only a few decimetres. The combination of active and passive cooling, together with conductive heat flux ~~regulation~~attenuation, performs best and allows excess energy to be fed into the local grid. ~~Findings~~ The findings of this study show the evolution of ground temperature and permafrost ~~evolution~~ at a representative alpine site under natural and thermally ~~stabilized~~ stabilised conditions, contributing to understanding the potential and limitations of ~~stabilization systems and formulate~~ stabilisation systems and formulating recommendations for optimal application.

1 Introduction

The effect of increasing air temperature on permafrost is the result of complex ~~,~~ and interacting processes occurring in different layers, including ~~canopy,~~ the grain size of rocks, the snow cover, and ~~active layers of soil~~the active layer. On the continental scale, between 2007 and 2016, the Arctic continuous permafrost experienced a warming of approximately 0.39 °C while the discontinuous permafrost warmed 0.20 °C (Biskaborn et al., 2019). In particular, this warming reached 0.8 °C per decade

at in the Svalbard archipelago , and 0.5 °C per decade in Russia (Smith et al., 2022). In the same period, globally global mountain permafrost temperatures increased by 0.19 °C (Biskaborn et al., 2019; Etzelmüller et al., 2020), responding to the raise rise of the atmospheric 0 °C isotherm (Kenner et al., 2024). Particularly the overall The general trend at some Alpine alpine mountain permafrost sites showed that warming at 10 m depth was 0.4 °C per decade between 1987 and 2009 (Haeberli and Gruber, 2009)(Haeberli and Gruber, 2009; Noetzli et al., 2024). These changes have led to an increase of the in active layer thickness (ALT) and shifted latitudinal permafrost limits northward (Biskaborn et al., 2019; Smith et al., 2022) and elevation limits to higher altitudes (Kenner et al., 2024)(Kenner et al., 2024; Noetzli et al., 2024). In Sweden, Greenland, and Svalbard, the ALT has been increasing since the 1990s (Strand et al., 2021).

Also , and similarly in mountain permafrost, ALT has been increasing since the 1990s, and in some places in where it has doubled in parts of the Swiss Alps it has even doubled in the 21st century (Smith et al., 2022; Swiss Permafrost Monitoring Network (PERM . At Schilthorn mountain in the Swiss Alps, annual average in-depth (Smith et al., 2022; Swiss Permafrost Monitoring Network (PERMOS) . On the Schilthorn mountain (Bernese Alps, Switzerland), annual average ground temperatures increased from -0.5 –0.5 to +0.03 °Cwhich resulted in doubling of the active layer depth (Swiss Permafrost Monitoring Network (PERMOS), 2024) , (Hauck, 2002). In the Swiss Stockhorn borehole , where the rate of temperature rise increased by a factor 4, the decadal warming rate reached , resulting in a tripling of the ALT (Hauck, 2002; Swiss Permafrost Monitoring Network (PERMOS), 2024) , while at the Stockhorn borehole (Valais, Switzerland), a four-fold acceleration in warming led to a decadal rate of +0.64 °C for between 2012 –and 2022 (Morard et al., 2024). At the Murtèl–Corvatsch , the permafrost borehole (Grisons, Switzerland), the warming over 18 years (1987-2006) was about years (1987–2006) reached approximately 0.5 °C at 11.6 m depth and 0.3 °C at 21.6 m depth (Harris et al., 2009a). Over , with continued increases over 35 years (1987-2022) of observation at Murtèl the temperatures at depth were increasing continuously, e.g., at 15 m to 20 m depth, from -1.8years (1987–2022) from –1.8 °C to -1.0 °C –1.0 °C at 15–20 m depth (Haeberli et al., 2023).

Thawing and warming permafrost and increasing ALT present a risk for built infrastructure to infrastructure foundations. It has been estimated that almost 70% of such infrastructure might infrastructure in the permafrost could be affected by 2050, with transport infrastructure (roads, railways, cable cars, etc.) being the most vulnerable and most abundant (Hjort et al., 2018) , (Hjort et al., 2022)(Hjort et al., 2018, 2022). A prominent Arctic example of infrastructure impacted by permafrost changes is the runway of the international airport at in Longyearbyen, Svalbard, where the thawing of ice-rich soils caused uneven settlement during the summer season, and the autumn re-freezing refreezing in the fall provoked heave formation, eventually leading to runway destruction ultimately leading to the destruction of the runway (Instanes and Mjureke, 2005). Besides transport infrastructure, over 1'000 settlements, and over 9'000 km of pipelines are located in areas subject to permafrost risk (Hjort et al., 2022). Failure of infrastructure might lead to environmental disasters as happened in May 2020 in Siberia, where 21'000 tonnes of oil were spilled in the Ambarnaya River causing devastating pollution with a total cost estimated at more than $2 billion (BBC News, 2020).

In mountain regions , such as the Swiss Alps, permafrost thawing also leads to noticeable impacts. In contrast to causes significant impacts. Unlike Arctic areas, mountain permafrost contains less excess ice. This small amount of ice acts like a natural "glue", stabilising slopes and cliffs. Its thawing weakens the static stability and therefore increases the risk of

rockfalls, landslides, and debris flows (Gruber and Haeberli, 2009), (Noetzli et al., 2003)in steep rock slopes contains little ice; its thawing allows water infiltration, which can lead to high pressures and rapid temperature increases. Infrastructure such as cable cars, houses, antennas , and avalanche protection systems etc. are put in danger, due to the mentioned risk and other destruction directly caused by permafrost thawing built on permafrost rock slopes can be destabilised (Duvillard et al., 2021). An impressive example is the 2017 large landslide Pizzo Cengalo rock avalanche in Bondo, Switzerland (Mergili et al., 2020), a compound event of cascading processes involving progression of a rockfall, to rock (or cascading event involving rockfall, rock-ice) avalancheand to a debris flow . Such processes avalanche, and debris flow (Walter et al., 2020). Such process chains are often directly related to changes in the cryosphere, e.g., linked to cryospheric changes such as glacial de-buttressing, retreating hanging glaciers, or vanishing thawing permafrost (Harris et al., 2009b; Haeberli et al., 2017). Ice-rich permafrost can also develop at the base of steep slopes in the snow avalanche and rockfall deposition zones (Kenner et al., 2019). Although these zones should be avoided in infrastructure planning (Bommer et al., 2010), this is not always possible. Ice warming and melting, combined with water infiltration, can lead to subsidence and creep, damaging the infrastructure on ice-rich ground.

All these challenges related to new or increased natural hazards and to of these challenges, whether from new or intensifying natural hazards or from the difficulties of building on mountain permafrost, require technical adaptation, including adaptations. These include the use of flexible, adjustable, or semi-mobile structures, advanced materialsspecially adapted building materials, and cooling techniques (Haeberli et al., 2010). Finding solutions for the (Haeberli et al., 2010; Bommer et al., 2010). The search for solutions for stabilisation of permafrost substrates in the currently affected regions, above, below, or around critical infrastructures, and wherever new constructions structures on permafrost are planned is becoming inevitable. Stabilisation of permafrost means primarily keeping it at sub-freezing temperatures and minimizing minimising the depth and dynamics of the ALT.

There are several different thermal stabilisation or thermal stabilisation and ground cooling methods currently applied worldwide. They applied worldwide, which can be divided into passive methods , i.e., these not requiring external energy during operation, (requiring no external energy) and active methods needing extra power supply. Common passive thermal stabilisation systems are based on the principle of increasing (needing additional power supply). Passive systems typically increase thermal resistance in the upper layer layers of the ground . Among these methods are using solar reflectors and shields (Qin et al., 2020), thermal insulation (Luo et al., 2018), and additional layers on top of the ground for protecting from solar radiation and net heat accumulation (Yinfei et al., 2016). The aim of these methods is protective layers to reduce the amount impact of net solar radiation, heat convection, and heat conduction conduction (Yinfei et al., 2016) above, within, and around the affected surface. However, these methods usually lack long-term effectiveness. To improve them, it has been recently proposed to regulate the heat transfer by Recent research proposes insulating the ground in summer to prevent heat penetration , and lifting the and lifting insulation in winter to allow effective ground for better cooling (Sharaborova and Loktionov, 2022). Other techniques are based on lowering the ground temperatures (Cheng, 2005) include so-called thermosyphones. The technology uses a sealed tube filled with a fluid (e.g., carbon dioxide, ammonia, or propane) to transfer heat from the soil to the atmosphere. The tube has two parts: an evaporator in the ground and a radiator above ground. When the ambient air temperaturedrops below ground temperature, vapour condenses in the radiator, reducing pressure and causing liquid in

the evaporator to boil and transfer heat to the radiator. The objective of thermosyphones is to lower the ground temperature through freezing during winter time and to ensure low temperatures during summer. Thermosyphones were initially proposed for freezing ground during wintertime beneath foundation pillars located approximately 6 meters below the seasonally thawed layer. This technology was also tested for protecting temperature, by seasonal in-depth cooling, (Cheng, 2005) to protect underground infrastructure (tunnels) in permafrost zones (Zhang et al., 2017) . A variation of thermosyphones was effectively implemented into highway embankments using heat pipes e.g. tunnels) (Zhang et al., 2017) and highway embankments (Tian et al., 2021). However, in some particular cases and for certain slope orientations there is still a risk they still face risks of surface deformation . In addition, due to the climate changethey are loosing their efficiency, because the winter becomes shorter and the frozen volume is not large enough to keep the ground stableand decreasing efficiency due to climate change, shorter winters, and shrinking frozen volumes.

In recent years, Although active cooling methods have undergone significant development, but their high cost due to the demand for substantial power has limited their been significantly developed in recent years, they are expensive due to power demands, limiting widespread use. Some progress has been made in the direction of using deep cooling in an active mode using solar energy (Hu et al., 2020). Their experiments demonstrated that active cooling is suitable for permafrost protection and that utilizing solar energy offers using solar energy (photovoltaic, PV) for active cooling in permafrost regions (Hu et al., 2020) , offering an economical solution for achieving field refrigeration without relying on grid powerin permafrost regions. This method could be improved upon by shielding from solar radiation and using by implementing solar radiation shielding and applying efficient energy redistribution and utilization. It has been shown in (Asanov and Loktionov, 2018; Loktionov et al., 2019) , that utilizing solar power use, with solar panels installed on embankments helps helping to achieve the combined effect of shielding from direct solar radiation and powering the cooling system . This method is based on a combination of passive and active thermal stabilisation techniques (Sharaborova et al., 2022a), where the solar panels act as sun screens, while simultaneously power the heat pump being the active component in the cooling process. (Asanov and Loktionov, 2018; Loktionov et al., 20 . The system uses pipes below the ground surface in which cooling liquid is circulating creating a cold (sub-zero) thermal layer, often referred to as subsurface pipes through which a cooling liquid circulates to create a sub-0°C thermal "barrier layer" preventing heat from the surface being conducted that prevents heat from penetrating deeper into the ground. The barrier layer, as introduced by (Sharaborova et al., 2022a; Loktionov et al., 2022)introduced by Sharaborova et al. (2022a) and Loktionov et al. (2022), serves to shield the cold ground against ambient heat penetration, unlike thermosyphons which cool massive volumes in the penetration of ambient heat, rather than cooling the large volumes of the ground at depth. To achieve this, the cooling pipes are placed parallel and close to the ground surface within the natural thawing layernear the surface. The effect of this method has been simulated for the lowland Siberian permafrost (Loktionov et al., 2022) using a 3D finite element method (FEM) package, specifically developed for permafrost soil calculations (Alekseev et al., 2018), and it has been lowland permafrost (Loktionov et al., 2022) and experimentally tested (Sharaborova et al., 2022b).

Permafrost in mountain regions poses extra presents additional challenges due to the settlement, deformation, and creep of the ground that can occur in complex , in complex ice-bearing terrain, requiring careful analysis, assessment , exploration of solutions, assessment and timely remedial measures to ensure maximum infrastructure lifetime (Bommer et al., 2010).

~~There are special construction methodsthat can be applied for mountain buildings , like cable cars and restaurants subject to deformation(Bommer et al., 2010). For example, a technique with flexible foundation systems can be used to carry out geometrical corrections when infrastructure subsides or creeps~~ the longevity of the infrastructure (Bommer et al., 2010). Special construction methods, such as flexible foundations for buildings subjected to deformation, can address subsidence and creep (Phillips et al., 2007; Harris et al., 2009a). Thermal stabilisation ~~methods~~techniques, including insulation ~~to mitigate heat transfer with air spaces or pressure-resistant materials like foam glass or~~ materials such as foam glass and extruded polystyrene, and passive cooling systems ~~like thermosyphonsare utilised~~ such as thermosyphons, are used in mountain permafrost construction, ~~though the latter are not widespread~~ although thermosyphons are less common in the Alps ~~(Phillips et al., 2007; Bommer et al., 2010)~~ (Phillips et al., 2007; Bommer et al., 2010).

To test and estimate the effect of thermal stabilisation methods on-site, experiments and monitoring are required. However, experimental designs are ~~time consuming~~ time-consuming and expensive. Modelling using numerical simulations is a good alternative to examine the impact and performance of cooling methods and to provide a better understanding of ~~thermal changes occurring in~~ the thermal changes that occur in the permafrost. Different models are used to simulate permafrost. Established physics-based 1D models such as the CoupModel ~~(Schaefer et al., 2014; Jansson and Karlberg, 2004; Marmy et al., 2013, 2016) and SNOWPACK (Lehning et al., 1999a)~~ (Jansson and Karlberg, 2004; Marmy et al., 2013; Schaefer et al., 2014; Marmy et al., 2016) , SNOWPACK (Lehning et al., 1999a) and CryoGrid (Westermann et al., 2023) are used to simulate mass and energy exchange processes in the soil-snow-atmosphere system. Such models have also been extended to cover wider areas as ~~1D distributed columns, as is the case for~~ distributed 1D columns, for instance, in Alpine3D, which ~~uses~~ is based on the SNOWPACK model ~~(Haberkorn et al.)~~ (Haberkorn et al., 2017) or a recent update of GERM (Huss et al., 2008; Farinotti et al., 2012) with a permafrost module (Pruessner et al., 2021). These models can also be used to simulate protective insulation methods. An example is the SNOWPACK simulation of ~~a~~ partial glacier protection using a geotextile cover (Olefs and Lehning, 2010) ~~which allows~~ or the assessment of snow farming (Grünewald et al., 2018) that allows us to examine in detail the energy exchange between different layers. Another example is the use of the ~~above-mentioned~~ 3D ~~FEM package~~ finite element method (FEM) package, specifically developed for permafrost ground calculations (Alekseev et al., 2018), to gauge the effectiveness of a thermal stabilisation method in permafrost (Loktionov et al., 2022).

The present study uses the SNOWPACK model to investigate the processes ~~occurring in~~ that occur in the permafrost during the application of passive and active thermal stabilisation methods at a selected mountain permafrost site. ~~The principal~~ Principal objectives are (1) to numerically examine the heat flux distribution in complex snow–ice–permafrost substrates and ~~on the contact border~~ at the interface with thermal stabilisation systems ~~,~~ and (2) to quantify the impact of thermal stabilisation on the ~~active layer thickness (ALT)~~ALT. We investigate how various cooling methods affect the long-term evolution of permafrost and its preservation in a cold state, and how they influence the thickness of the active layer, in combination with thermal stabilisation approaches. The results are expected to help ~~to~~ assess the pros and cons of different thermal stabilisation methods for ~~permafrost~~ protection and preservation of permafrost. The numerical studies allow the creation of an integrated view of the technology behaviour and help to adapt it for in-situ application.

This study focuses on numerically evaluating the performance of thermal stabilization methods using borehole data at Schilthorn The objective of this study is the numerical evaluation of the performance of engineering methods for thermal stabilisation of alpine permafrost and its sensitivity to different design parameters. The study uses data from the Schilthorn Mountain borehole, Switzerland, a high-altitude high-elevation site representative of alpine permafrost regions. By analysing their impact on key variables such as ground temperature, heat fluxes, and ALT, we aim to provide insights into information on the efficacy of these measures and their potential of improving to improve the resilience of permafrost against atmospheric warming. The findings contribute to optimizing optimising engineering practices in permafrost regions and addressing knowledge gaps in permafrost thermal management. The results obtained are specific for the particular site conditions at Schilthorn, because parameter selection was carried out to best reproduce the measured temperature profile evolution for the natural situation. However, results can be considered representative for a range of conditions typical of alpine permafrost. Furthermore, research on mountain permafrost stabilisation remains limited. As a result, this study offers new insights, but also highlights the need for further research to make wider comparisons and draw broader conclusions.

2 Modelling with SNOWPACK

Here, we build upon on previous research employing the SNOWPACK model for permafrost studies (Pruessner et al., 2021, 2018; Luethi et . The model was initially (Luethi et al., 2017; Pruessner et al., 2018, 2021). Initially, the model was developed for avalanche warning (Lehning et al., 2000) and it computes the computes 1D heat transfer, water transport, vapour diffusion, and mechanical deformation, including new snow, wind drift, and snow ablation. It includes a description of soil layers describes the layers of the ground (Luetschg et al., 2008) where the physical properties (thermal conductivity, heat capacity, density) remain constant over time (Pruessner et al., 2021). SNOWPACK includes offers both a simple bucket water transport model (Lütschg, 2005) and an advanced Richards water transport model (Wever et al., 2014, 2015) to simulate water transfer the transfer of water from the snow cover to the underlying substrate. In the current study, we use a simple the bucket scheme, which allows us to set directly specify the fixed substrate volumetric content for each soil layer. In contrast, the Richards scheme requires specifying the layers and not to specify the grain size of the soil ground layers to determine the water retention properties of the soil. The bucket model in SNOWPACK SNOWPACK bucket model is computationally very efficient and was tested for various mountain permafrost sites. SNOWPACK also allows for the incorporation of artificial materials on the surface as an additional model layer. This feature has been used to successfully model geotextile-covered snow (Olefs and Lehning, 2010)showing a , showing good agreement between the modelled and experimental observed temperature profile of artificially conserved snow. This model feature feature of the model is also used in the present work to represent the inclusion of thermal insulation material.

Heat sinks and -sources sources can be represented in the model by an advective heat flux formulation (Luethi et al., 2017). This capability can be used to heat or cool any layer, including the soilground, and model, for example, talik formation in the permafrost (Luethi et al., 2017). Based on these previous applications of SNOWPACK, the model is considered to be well suitable for studying the effects of thermal stabilisation systems in mountain permafrost. In this study, we used SNOWPACK

Version 3.7 to model the effects of cooling pipes in the ground. We introduced an optional feature to the model to allow for a representation of the artificial cooling as if it ~~was~~ were installed on the site, and to control heat ~~advection from the~~ transfer between the ground and the cooling pipes. The modified version of the model includes a switch to regulate temperature and ~~remove the~~ to remove heat from the ground by ~~activation~~ activating the advective heat mode. ~~The user sets a temperature limit~~Upper and lower temperature limits can be specified. When the ground temperature ~~reaches~~ has cooled to the set threshold, the cooling system ~~turns off, in the model it means advective heat is deactivated. Otherwise, if the temperature of the ground is too high - above the established threshold -~~ is turned off. If the ground temperature passes the specified upper limit, the cooling is activated ~~. However, due to the 1-D formulation of the model, exact simulation of the temperature along the cooling pipes is not possible. The model prescribes with a constant temperature in the pipe, not considering the fluid temperature difference at the entrance and exit of the pipe due to heat conduction to the surrounding ground as would be the case in a 3-dimensional situation. Another approximation is that the calculation of the power required for cooling is simplified, and only effective when solar radiation is available. A more advanced way would be to monitor the cooling, and adapt the power supply according to the conditions of the ground and the solar power production. The current state of the model allows us to assess the thermal stabilisation potential of a system and show its effects when applied at a permafrostsite. However, for a more detailed study of the stabilisation application further model refinement is still required. This includes minimizing the current approximations and simplifications, aiming for a representation that better captures practical behaviour.~~

~~The rational of using SNOWPACK for modelling thermal stabilisation in permafrost compared~~ again.

The decision to use SNOWPACK to model thermal stabilisation in permafrost, in contrast to previous work ~~(Loktionov et al., 2022) is the better~~ by Loktionov et al. (2022), is motivated by its representation of snow ~~, ground parameters, and the permafrost temperatures during the entire simulation . In Loktionov et al. (2022),~~ dynamics, ground thermal properties, and permafrost temperature evolution over the full simulation period. In Loktionov et al. (2022) a 3D model ~~was used with third-type boundary conditions at the soil surface, where heat fluxes were calculated using air temperature and heat transfer coefficients based on wind speed. However, in SNOWPACK , boundary conditions can be set using Neumann conditions, directly calculating the heat fluxes at the surface . It also avoids the connection with surface temperature , which will be changing with the application of the~~ uses a type III boundary condition, which can be beneficial for permafrost modelling but relies on a simplified treatment of surface processes. The model used by Loktionov et al. (2022) is more practical for engineering reasons, especially when the ground is under the thermal influence of the infrastructure and constructions. SNOWPACK is more aligned with scientific research goals, given its comprehensive treatment of snow and soil physics. The advantage of SNOWPACK is that it presents a full set of surface fluxes, including a wide choice of stability corrections. This approach allows the surface temperature to evolve naturally based on the energy balance and the applied cooling methods. These boundary conditions ~~provides a more~~ provide an accurate representation of the heat exchange between the ground and the atmosphere, with a ~~better~~ representation of the heat flux at the soil-atmosphere interface. ~~Even if the model from Loktionov et al. (2022) uses the third-type of boundary condition~~This is especially advantageous when measured surface temperatures are unavailable or unreliable. Moreover, the 3D model comes with higher computational demands, which can ~~be benefit for permafrost modelling, the advantage of SNOWPACK is that it presents a full set of surface fluxes, including a wide choice of stability corrections for turbulent fluxes.~~

In addition, limit its practicality for multi-year simulations or sensitivity analyses. In comparison, SNOWPACK enables the rapid simulation of long periods with detailed vertical resolution, making it more suitable for exploring a range of scenarios and parameter sensitivities. SNOWPACK enables the detailed representation of every model layer including temperature, heat flux, and the possibility of monitoring the output of the permafrost parameters . Another advantage is the possibility of modelling multi-year periods in very short time, the inclusion of radiation effects on (ground temperatures, volumetric water content, bulk density, thermal conductivity, heat capacity, temperature gradient, etc.). Another notable difference lies in the treatment of the ground, and the possibility of controlling the albedo effectssnow cover. SNOWPACK can simulate the evolution of the snow cover either by prescribing measured snow height values or by calculating the new snow depth based on observed precipitation and air temperature. When the snow cover is prescribed from measured snow depth values it takes into account local drifting snow, since that is included in the snow depth measurements. The 3D model of Loktionov et al. (2022) uses a constant albedo value for snow, suggesting a simplified representation. SNOWPACK includes a physically based multi-layer snow model, simulating snow accumulation, compaction, metamorphism, and albedo evolution. This more realistic snow treatment is critical in permafrost studies, as snow insulation is a dominant control on ground thermal regimes. SNOWPACK fits the goals of this study because it matches the available data, offers clear transparency, accurately represents snow processes, and runs efficiently.

3 Study Description of study site and data

In this study, we use borehole used the temperature data from the PERMOS mountain permafrost site SchilthornSchilthorn PERMOS permafrost borehole site, canton Bern, Switzerland (46.558292 N, 7.834626 E, 2923 m a.s.l.) (Swiss Permafrost Monitoring Network (PERMOS), 2024). This site is representative for many locations of alpine permafrost We selected this site because it is representative of many alpine permafrost locations and because the nearby infrastructure will could be affected by permafrost thaw. Over During the past decade, the ALT at this site has doubled (Hauck and Hilbich, 2024). By studying Schilthorn during a period when the ALT was thinner and before these significant changes occurred, we gain valuable insights into the dynamics of mountain permafrostHauck and Hilbich (2024) indicating a general deepening of ALT from 4–5 m before 2008 to 5–7 m by 2016, with subsequent increases leading to 13 m after the extremely hot summer of 2022. This approaches the threshold (about 14 m) beyond which full winter refreezing may no longer be possible. The ALT thickening causes direct risks to challenges for the infrastructure, such as cable car foundation, hiking trails, and mountain huts. Permafrost thaw can lead to local cable car foundations, pylons, and buildings. The thaw of the permafrost can cause slope instabilities, rockfalls, or subsidence. Indirectly, this results in economic losses due to repair costs and danger to recreation activities. These risks are especially significant for infrastructure , destabilising building foundations, particularly when located on steep or unstable slopes. These insights risks are also applicable to similar Alpine sites with cable car infrastructures infrastructure or other facilities, such as for example, the Zermatt / Matterhorn area in Switzerland (Weber et al., 2017), or the Chamonix/Mont Blanc region in France (Duvillard et al., 2021).

Figure 1 shows the location of the site with respect to the spatial permafrost distribution and solar radiation level. Meteorological and borehole stations from distribution of permafrost, indicating ground temperatures and ice content, and average yearly totals

of solar radiation. Meteorological stations and borehole sites (Table 1) are shown in Figure 1 on the right panel. The observational permafrost temperature and atmospheric data sets of this site are ~~largely sufficient~~ well suited for modelling purposes, as they include sufficiently long periods of meteorological forcing and permafrost temperature and distribution.

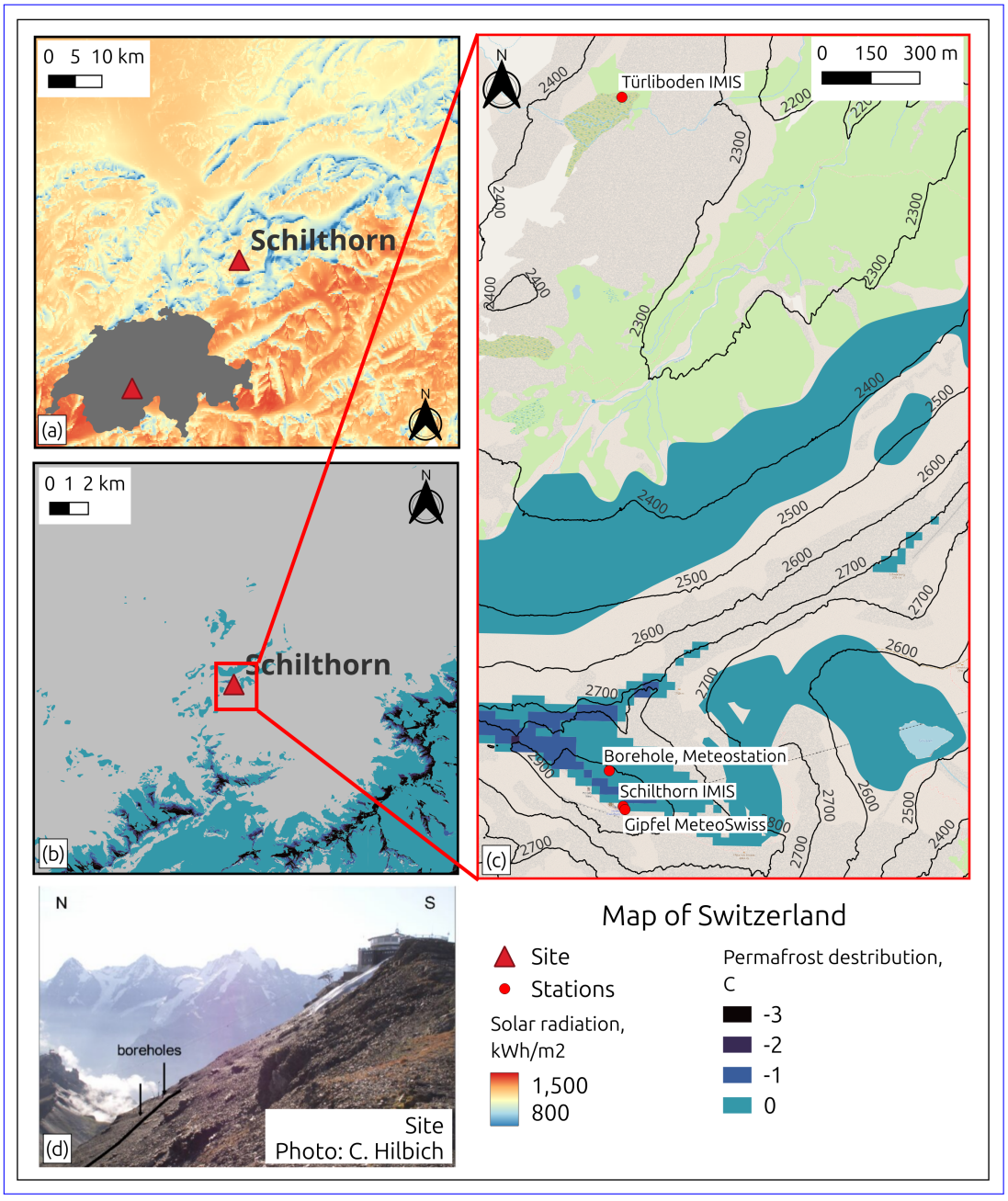

Figure 1. ~~Map~~ (a) Average yearly totals of ~~Switzerland indicating~~ solar radiation (Solargis, 2020) showing the Schilthorn ~~study~~ site on an area map and on a map of Switzerland (~~red triangle~~gray shaded). ~~The map shows~~ , (b) permafrost distribution adapted from ~~(Kenner, 2018)~~ Kenner (2018), (~~spectrum from dark blue to light blue~~c) ~~, and yearly averaged solar radiation (Solargis, 2020)~~ zoom into panel (~~spectrum from blue to red~~b) ~~. The site is shown on~~ indicating the ~~bottom left (Hilbich, 2010)~~ site of Schilthorn borehole and ~~the~~ surrounding meteorological stations ~~' (green circles) position from~~ Table 1, and (d) picture of borehole site and Schilthorn summit (Hilbich, 2010). Coordinates are based on ~~the right~~UTM Zone 32T (EPSG:32632) for Switzerland. Schilthorn, E: 419500, N: 5158000.

Table 1. Meteorological and borehole data used for modelling. IMIS denotes Intercantonal Measurement and Information System.

Station	Coordinates	Data used
Schilthorn borehole (Swiss Permafrost Monitoring Network (PERMOS), 2024)	46.558 N, 7.835 E 2900 m a.s.l.	Borehole temperatures at depths (m): 0.2, 0.4, 0.8, 1.2, 1.6, 2, 2.5, 3, 3.5, 4, 5, 7, 9, 10, 11, 13
Schilthorn meteo station (Hoelzle et al., 2022; Swiss Permafrost Monitoring Network (PERMOS) and Hoelzle, 2021)	46.558 N, 7.835 E 2900 m a.s.l.	Air and surface temperature, relative humidity, wind speed, radiation (all components), snow depth
Schilthorn IMIS	46.557 N, 7.835 E 2996 m a.s.l.	Air temperature, wind speed, relative humidity
Türliboden IMIS	46.577 N, 7.835 E 2332 m a.s.l.	Reflected short-wave radiation, surface temperature, snow height, precipitation
Gipfel MeteoSwiss	46.557 N, 7.835 E 2970 m a.s.l.	Wind speed

~~IMIS: Intercantonal Measurement and Information System~~

The borehole temperatures were obtained from the Schilthorn SCH_5198 borehole operated by PERMOS (Swiss Permafrost Monitoring Network (PERMOS), 2024). The borehole was established in 1998, it is 13 m deep and temperature is presently still measured. The ground temperature averaged over 13 m depth and over the period 1998 to 2025 is ~~still active. For the~~ 0.02 °C (Swiss Permafrost Monitoring Network (PERMOS), 2024), the temperature range at the profile base is from -0.88 °C to 0.58 °C, and the ALT changes from 4.4 m to 13 m. For simulations, we used atmospheric data (Table 1) from the PERMOS meteorological station next to the borehole ~~(Hoelzle et al., 2022; Swiss Permafrost Monitoring Network (PERMOS) and Hoelzle, 2021) .~~ for the years 2000 to 2017 (Swiss Permafrost Monitoring Network (PERMOS) and Hoelzle, 2021; Hoelzle et al., 2022). Long-term observations Hoelzle et al. (2022) state that the mean air temperature observed at Schilthorn (1998-2018) is -2.60 °C, the mean snow height – 0.87 m, and the snow season usually lasts from October to June (Swiss Permafrost Monitoring Network (PERMOS) and Hoe . Due to the presence of gaps~~the data was~~ , the data were completed with data ~~of the nearest~~ from the closest stations of the Intercantonal Measurement and Information System (IMIS) ~~stations and MeteoSwiss meteorological stations~~ and MeteoSwiss network (Table 1) for the same time period. To reduce ~~the~~ bias related to the ~~used input data~~ input data used, correlations between the Schilthorn meteorological station and the other stations were calculated, and existing gaps were filled based on the ~~obtained regression coefficients~~ regression coefficients obtained. The remaining gaps were filled ~~with the MeteoIO interpolation and generation~~ using the MeteoIO data generation and interpolation functions (Bavay and Egger, 2014).

We ~~set-up the model to correspond to observational data~~ set up the model using the following set of parameters: volumetric ice, water, substrate, and voids content of the ground~~:~~ , substrate density, thermal conductivity, and heat capacity. Based on the available data from the borehole temperature measurements and previous modelling experience (Marmy et al., 2013; Ekici et al., 2015; Wag , we use the substrate parameters listed in Table 2. The site is free of vegetation and the substrate consists of ~~deeply weathered dark limestone at~~ dark, deeply weathered limestone on the surface of mainly sandy and ~~gravelly~~ gravel debris of several ~~meters~~

depth, which lies metres in depth, lying over strongly jointed bedrock (Zappone and Kissling, 2021). The required initial conditions initial conditions required for the model were chosen to represent rocky ground, without specifying particular grain sizes for different layers. Based on the available borehole temperature measurements data and previous modelling experience (Hoelzle et al., 2022; Marmy et al., 2013; Ekici et al., 2015; Wagner et al., 2019), it is assumed that the substrate parameters are those shown in Table 2. The top SNOWPACK requires appropriate initialisation; however, a spin-up may not be necessary if the ground temperature profile is initialised using the corresponding observational data. Each layer was divided into grid cells with a vertical extent of 0.1 m. The upper layer consists of well-drained loose rock (talus) and thus has a lower water content and moderate porosity, which explains the lower heat capacity required to reproduce the temperature distribution. Below this, the heat capacity increases representing the presence of an active layer, which is indicated by long spring and autumn zero-curtains (Swiss Permafrost Monitoring Network (PERMOS), 2024). The zero-curtain effect happens due to the slowed occurs as a result of the latent heat release/consumption during the phase transition (thawing or freezing) in the active layer. At this time, the ground temperature remains near 0ºC close to 0 °C over an extended period, meanwhile, while the air temperature may vary significantly. At depth, the standard values for limestone are used. The values for density and thermal conductivity are determined according to the given substrate stratification. The geological map (Zappone and Kissling, 2021) indicates that the site has a limestone bedrock on this site in depthand the at depth, with sandy and gravelly debris in upper layers, justifying gravel debris in the upper layers. This justifies the use of the corresponding values recommended recommended corresponding values for this type of ground (Table 2).

Table 2. Parameters of geological substrate for the Schilthorn site simulations.

Depth, m	Volumetric content (ice, water, void, substrate), %	Density, kgm^{-3}	Thermal conductivity, $W\,m^{-1}\,K^{-1}$	Heat capacity, $J\,kg^{-1}\,K^{-1}$
0-2.5	0; 20; 21; 59	1600	2.2	700
2.5-5	5; 20; 6; 69	2000	2.7	1000
5-13	10; 0; 0; 90	2700	3.0	900

4 Model simulations

To understand the processes happening that occur in permafrost soils, different configurations of numerical simulations were employed, first simulating natural conditions without engineered modifications and then applying different thermal stabilisation methods. These simulations are numbered for easy reference and summarised in Table 3. The simulations have been run from for the period June 2000 until to January 2017. The This time frame was selected as it precedes the significant observed increase in ALT, aligns with available meteorological data, and represents long-term observations of permafrost temperatures at the site. Focusing on the period before the major increase in ALT provides a baseline reference and highlights how early intervention could have prevented subsequent degradation, serving as a cautionary example for similar at-risk sites. Starting

simulations in June avoids defining an initial snow cover and related uncertainties in its properties. The simulation of this period allows reconstructing the impact from thermal stabilisation methods and analysing the re-establishment of new temperature equilibrium within the ground, while preserving permafrost and delaying an increase in ALT at the site. This also allows to extrapolate obtained results to other similar permafrost sites. The model runs at an hourly time interval using meteorological forcing at 2~~m height and the model output both have an hourly time step~~ m above ground. This is a temporal resolution necessary to represent fast-changing weather conditions and to simulate their impacts, for instance, on the energy balance and its various heat fluxes. For coherence, the model uses the same 1-hour time step. Internally, the model interpolates the hourly forcing on a 15-minutes time step (accomplished by the MeteoIO library (Bavay and Egger, 2014)) to avoid abrupt step changes and to obtain higher temporal resolution simulations.

Table 3. Overview of model simulations.

Exp.#	Description of model configuration
1	Natural conditions (reference case)
2	Shading of the surface by solar panels
	2.1 Shading from wind (wind speed decreased by 70%)
	2.2 Shading from liquid precipitation (liquid precipitation is neglected)
	2.3 Shading from snow (snow is neglected)
	2.4 Shading from direct short-wave radiation (direct short-wave radiation is neglected)
	2.5 Net effect of 'shading' (all parameters from 2.1-2.4 participate)
3	Thermal insulation at the surface throughout the year
4	Seasonal thermal insulation (heat flux attenuation during summer)
5	Active cooling (cooling pipes alone)
6	Active and passive cooling (cooling pipes and shading)
7	Active and passive cooling (cooling pipes and shading), 50% of PV power for cooling
8	Active and passive cooling (pipes and shading), 10% of PV power, seasonal thermal insulation

4.1 Natural conditions

Numerical simulations of natural conditions were carried out as a reference case ~~and~~ (Exp. #1, Table 3) to evaluate the performance of the model compared to the measured temperatures from the borehole. These simulations, combined with the study of the modelled and measured substrate parameters at this site (Pellet et al., 2016; Scherler et al., 2010; Marmy et al., 2016), allowed ~~for selecting~~ the right setting ~~for optimizing~~ to optimise the agreement of the ~~SNOWPACK~~ modelled temperature distribution and the measured ~~borehole temperature data . Albedo~~ temperature data from the borehole. The soil albedo was set to 0.15 ~~for soil~~ and we used the ~~Schmucki et al. (2014) albedo parametrization for snow~~ snow parametrisation of

Schmucki et al. (2014), which estimates the albedo based on the time elapsed since the last snowfall, grain size and liquid water content (Lehning et al., 2002). The roughness length was set to 0.05 m ~~owing to~~ accounting for the rocky surface. We used the ~~Holtslag and Bruin (1988)~~ Holtslag and Bruin (1988) correction model for atmospheric stability, which shows ~~a good performance over~~ good performance on snow surfaces (Schlögl et al., 2017). ~~To facilitate modifications during the thermal stabilization experiments we~~ We forced the model with available snow depth measurements from the site, avoiding the calculation of snow depth from precipitation data (Table 1) which includes only rainfall. In this way, we implicitly take into account local snow drift, since its effect is integrated in the observed snow depth. We force the model with incoming short-wave radiation~~mode~~, while the other energy balance components are computed by the model based on available meteorological forcing data (air temperature, wind speed, relative humidity, ~~incoming short-wave radiation, snow height,~~ snow depth, and liquid precipitation equivalent~~and bottom ground temperature)~~) as well as the temperature at the base of the model domain for a full ~~surface~~ energy balance assessment. At the surface, a Neumann boundary condition has thus been applied. The observed surface temperature data (Table 1) ~~is not directly used~~ are not used directly as input for the model simulations~~but serves for comparison of~~ , but serve to compare the model output ~~to the measurements for consistency~~ with the measurements as a consistency check. At the base of the ~~simulation~~ model domain, a Dirichlet boundary condition is used, prescribing borehole temperature measurements ranging from -0.9 °C to -0.1 °C.

We quantitatively compared the model output with the borehole temperature measurements using standard statistical analysis such as bias, root mean square error (RMSE) ~~,~~ and correlation (Pearson coefficient) at different depths for monthly mean averages and for the whole time series. ~~Additionally~~In addition, we compared the mean values and standard ~~deviation~~ deviations for different model setups with observations. The ~~best performance setup~~ setup that produced the best performance was chosen as a reference case ~~.~~ (Exp. #1).

4.2 Thermal stabilisation modelling experiments

4.2.1 Shading of the surface

~~Surface shading~~

Surface shading from structures above the ground protects the soil from direct solar radiation, snow, and liquid precipitation. It also affects the wind speed near the ~~soil. The effect of the snow accumulation is that it works as a natural insulation, therefore, in winter it doesn't let the heat be extracted from the ground, and limits natural cooling (Wang et al., 2019). As for the precipitation, it negatively affects by increasing the ALT which accelerates permafrost degradation (Zhu et al., 2017; Wang et al., 2021) . Wind speed decreasing/increasing can affect as positively as negatively on permafrost, impacting the heat transfer, snow redistribution and moisture content, which in turn can either protect or accelerate permafrost degradation (Zhao and Yang, 2022) . We simulated shading using solar panels positioned above~~ ground~~level~~. We simulate the shading of solar panels placed above the ground, exceeding the height of the snow cover, as proposed by ~~(Loktionov et al., 2022)~~Loktionov et al. (2022). To quantify the impact of shading ~~from~~ of various parameters individually and ~~combined~~in combination, we conducted experiments in two stages. In the first stage, we investigated the effect of each of the following parameters independently ~~from~~ of each

other: (1) wind speed decreased by 70%; (2) the ground completely protected from snow and liquid precipitation; (3) ~~no direct component of the~~ only the diffuse component of incident short-wave radiation~~leaving only the diffuse component~~, which is derived from the reference case SNOWPACK simulation under natural conditions. In a second step, all parameters were modified simultaneously, simulating the combined effect on heat transfer and vertical temperature distribution.

Snow accumulation works as natural insulation; therefore, in winter it prevents heat loss from the ground and limits natural cooling (Wang et al., 2019). Liquid precipitation has a negative impact as it increases the ALT which accelerates permafrost degradation (Zhu et al., 2017; Wang et al., 2021). Changes in wind speed can have a positive or negative impact on permafrost, affecting heat transfer, snow re-distribution and moisture content, which in turn can slow or accelerate permafrost degradation (Zhao and Yang, 2022). Based on these known impacts, we designed our simulations to test the effect of neglecting individual components: wind, solid and liquid precipitation, and direct solar radiation to better understand their respective roles in permafrost thermal dynamics.

The choice of ~~these parameters was partly~~ parameters (1) and (2) was based on previous ~~experiences from modelling the thermal stabilization effect~~ modelling results investigating thermal stabilisation (Loktionov et al., 2022). However, ~~in this study the solar radiation~~ Loktionov et al. (2022) instead applied a solar radiation value that was decreased by 95% from global horizontal irradiance (GHI). In the present study, we can revert to the modelled components of direct and diffuse solar radiation. ~~In the case of the ground being shaded by the solar panels, we are neglecting the direct radiation component.~~ Using only the diffuse solar radiation component is a simplified and idealised case, which allows to reproduce the effect of the solar panels on ground temperature distribution, without applying an additional empirical coefficient. Removal of the direct solar radiation component accordingly reduced the radiative heat flux from the atmosphere ~~accordingly~~(Liu and Jordan, 1960; Olson and Rupper, 2019; Li et al., 2020). ~~The real effect of the~~ In reality, solar panels may ~~bring a bigger/smaller~~ have a different impact on the solar radiation ~~intensity~~ reaching the ground beneath solar panels depending on the spacing and inclination of the panels. The numerical tests with these assumptions allow us to model the impact ~~from~~ of the solar panels placed above the ground~~,~~; however, for more accurate analysis, ~~in-situ~~ in situ experiments are required. ~~Test~~ The test results will show the impact of each change on thermal stabilisation ~~, its efficiency , and the seasonality. During the second stage, all parameters were modified simultaneously. This experiment simulates the total effect of the heat transfer and vertical temperature distribution with the application of the shading method. The objective of this experiment is to allow more efficient surface cooling in winter by heat loss to the atmosphere and by reflecting solar radiation.~~ and its efficiency over the seasons.

4.2.2 Thermal insulation

~~We also consider the situation of the ground being~~

We also model the ground covered with thermal insulation material. We simulate the presence of a 50-100 mm thick polystyrene slab with a thermal conductivity of 0.033 $\mathrm{W\,m^{-1}\,K^{-1}}$, a density of 28 $\mathrm{kg\,m^{-3}}$ and a heat capacity of 1500 $\mathrm{J\,kg^{-1}\,K^{-1}}$ to reduce heat transfer from the atmosphere to the ground (Loktionov et al., 2022). ~~Test simulations showed that a thickness of 50-100 mm is needed to have a sufficient insulating effect. It additionally increases the albedo, reflecting more solar radiation from the ground. This was implemented in the model~~The thickness range was chosen such that efficient heat control in the

context of this study was possible. We also simulated a thinner slab, which was found to be insufficient to reduce heat transfer. The insulation material also increases the surface albedo. In the model, this was implemented as an additional layer (styrofoam) at the top of the soil to preserve ~~the cold~~ low temperatures at depth. Similarly to the ground layers (Section 3), the thermal insulation layer and layers between 0 m and 0.2 m were divided into grid cells of 0.05 m for both 50 mm and 100 mm material thickness. The albedo of the ~~isolation material is assumed to be 70%~~ insulation material is set at 0.7, representative of white styrofoam with a high-albedo reflective coating (Ramamurthy et al., 2015; Qiu et al., 2018; Chen et al., 2020) and similar to a snow cover. Two particular cases are investigated: (1) insulation present all year round ~~,~~ and (2) insulation ~~placed on the ground~~ present from the beginning of June until the end of October (under snow-free conditions) and lifted from November until the end of May to ~~favour~~ allow the natural cooling process. In (1), the insulating material protects the ground from direct contact with snow and rain. However, both ~~precipitation types still continue to~~ types of precipitation accumulate on top of the protection layer, which is considered in the simulation. ~~At this step, we also studied the impact of thermal insulation thickness, by showing different cases of thermal insulation material thickness (50 mm, 100 mm).~~ The objective of (2) is ~~monitoring~~ to regulate the heat flux ~~regulation (Sharaborova and Loktionov, 2022) by~~ (Sharaborova and Loktionov, 2022) by shielding during summer and favouring natural cooling in winter~~and preserving the low soil temperatures in summer~~. The advantage of (2) is the combination of the shading effect of the solar panels (~~see~~ Section 5.2.1) with the ground insulation material. This ~~term~~ approach has been introduced in the ~~method description (Sharaborova and Loktionov, 2022), and relates to the regulation of~~ description of the method (Sharaborova and Loktionov, 2022) and is related to the attenuation of the conductive heat flux and temperature. ~~The heat flux regulation effect is achieved in this invention for the~~ In this configuration, heat flux attenuation and prevention of permafrost thawing ~~without~~ are achieved without an external power supply. The method stabilises frozen ~~rocks~~ ground by insulating the soil in warm seasons by protecting the ground from solar radiation ~~,~~ and precipitation, and by limiting convective heat transfer. Elevating the insulation above snow cover in winter helps to use natural air circulation for cooling.

4.2.3 Thermal stabilisation with active cooling

~~This experiment~~

This experiment (Exp. #5, Table 3) simulates the case of thermal stabilisation using a solar-powered heat pump (Sharaborova et al., 2022a). The system combines the previously described passive protection (Section 4.2.1), where ~~the~~ solar panels act as sunscreens ~~, and at the same time also power~~ and as a power source for the heat pump ~~for~~ cooling the ground through cooling pipes. The latter are modelled by implementing ~~an sink term which~~ a sink term at the level of the pipes that corresponds to the energy ~~produced by solar panels and available for cooling the soil by means of the heat pump and keeping the temperatures around ground pipes at temperatures lower than~~ supplied by the solar panels keeping the ground temperatures around the pipes below 0 °C.

~~Based on previous studies modelling~~ Similarly to previous studies simulating the application of a thermal stabilisation system ~~application~~ (Loktionov et al., 2022), we model ~~the cooling pipes by~~ cooling pipes applying a negative advective heat (q_{adv}) in the ~~concerned layers below ground~~layers concerned. The advective heat is implemented in the following way: First, the energy obtained from the solar panel is calculated using ~~the~~ incoming short-wave radiation (ISWR), the solar panel surface

area ($A = 1\,\mathrm{m}^2$), and the photovoltaic ~~(PV)~~ conversion efficiency ($\eta = 10\%$), as detailed in Equation (1). Then, this power is applied ~~as coolingpower~~to cooling, using the cooling energy efficiency rate (EER), Equation (1), which is related to the coefficient of performance (COP) for cooling machines and for heat pumps, according to Equation (2), and depends on the ambient (atmospheric) temperature~~, as evident in Equation (1)~~. Equation (1) is ~~adopted from the previous study of this thermal stabilisation method (Loktionov et al., 2022)~~adapted from Loktionov et al. (2022), the coefficients ~~there are obtained based on the characteristics of the equipment . This relation of parameters is different depending on the model and design of the heat pump. Finally~~are specific to the equipment used. Finally, to determine the advective heat ~~that is~~ applied in the model, the cooling capacity is divided by the volume of the ~~cooling application~~layer that contains the cooling pipes. This procedure is described using the following equations:

$$q_{\text{adv. heat}} = \frac{\text{ISWR} \cdot \eta \cdot A \cdot \text{EER}}{V} \tag{1}$$

$$\text{EER} = 4.8 - 0.12 \cdot T_a \tag{2}$$

$$\text{EER} = \text{COP} - 1 \tag{3}$$

~~The advective~~ Advective cooling was applied ~~in the model~~ for the months of April to October. The cooling pipes are integrated into the model ~~as advective cooling at~~ in a layer from 20 cm to 22.5 cm (the diameter of the pipe is 25 mm), ~~and are~~ cooling this layer to a minimum temperature of $-7.5\,^{\circ}\mathrm{C}$, which corresponds to the mean temperature of ~~coolant expected~~ the coolant circulating in the pipes ~~. The active cooling from the~~ (Loktionov et al., 2024a). To accurately represent this process, the grid cell thickness for layers between 0 m and 0.8 m was refined to 0.005 m. Active cooling from pipes creates a thermal barrier layer of a cold (frozen) slab inside the ground ~~protecting~~ that protects the permafrost in summer from heat conducted from the surface deeper into the ground. ~~Experiment 1~~ Exp. #5 (Table 3) applies active cooling ~~with pipes only but~~ alone without shading the soil with solar panels. ~~Experiment 2 combined both elements, i.e.,~~ Exp. #6 (Table 3) combines passive and active cooling. ~~We consider that the surface of solar panels is equivalent to the cooling surface as 1:1, in both experiments~~In both experiments, the cooled area corresponds exactly to the area of the solar panels. However, in real life, this relation will be more complex, depending on the time of ~~the day, slope orientation~~day, local topography, ground parameters, etc. Later in this study, we ~~examined also the cases with partial energy use from the solar panel (Section 5.3), when only part~~ also examine cases in which only a portion of the energy ~~(from the total production by solar panels)~~ from solar panels is reserved for ~~the cooling~~ cooling (Section 5.3).

5 Results and discussion

~~Before discussing the specific results of the different simulations, we want to reiterate the main objective of this study being the evaluation of the performance of engineering methods for thermal stabilisation of alpine permafrost and its sensitivity on different parameters. Also note that the results are specific for the particular site conditions at Schilthorn, although they can~~

be considered representative for a range of conditions typical for alpine permafrost regions, and that parameter calibration was carried out to best reproduce the measured temperature profile evolution for the natural situation.

5.1 Natural conditions

The simulated ground temperature evolution together with the evolution of ground temperature and observed snow depth at the Schilthorn site is shown in Figure 2 for the entire observation period from 2000 to 2017. The seasonal active layer outlined with By studying Schilthorn during a period when the ALT was thinner and before significant changes occurred, we gain valuable insights into the dynamics of mountain permafrost. The seasonal ALT is indicated by the 0 °C isotherm is evident and the ground temperature at depth and the temperature at the base of the model domain corresponds to the measured permafrost temperature in the borehole. We can also note an increase of the ALT over also observed an increase in ALT over the years from about 5 m to almost 87 m. In natural conditions, a realistic computation of the ground heat flux follows from depends on an accurate representation of the snow height depth as shown in Figure A1, where the modelled and measured snow align closely for most of the winters. For some periods, the measured snow depth is below the simulatedone , indicating that the model would underestimate meltor erosion underestimates compaction, melt, and erosion (Lehning et al., 1999b). Figure 3a indicates that the modelled temperatures are slightly higher than measured. However, the monthly averaged average difference for the whole period of simulation entire simulation period never exceeds 1 °C. Figure 3b indicates that the model and the observations are comparable with similar long-term mean temperatures and standard deviations in all model layers evidenced by the correlation coefficients larger throughout the vertical profile, evidenced by correlation coefficients greater than 0.8in all layers, except for the middle layers, notably at the especially at depth around 5 m, where the coefficient drops to almost 0.6. This depth corresponds to the ALTwhere the ALT sensitively depends on small changes in temperature , where even small temperature variations (on the order of a tenth of a degree) resulting in relatively large fluctuations in the position of the ALT (Marmy et al., 2016). can cause significant fluctuations in its position (Marmy et al., 2016).

5.2 Thermal stabilisation experiments

5.2.1 Shading of the surface

We studied the impact of shading on the ground temperature in several experiments, isolating the effect of individual elements as described in Section 4.2.1 by and comparing the simulations with the averaged natural conditions (Figure A2) . Modification as described above. Reduction of liquid precipitation by sheltering effects results in the smallest temperature changes in the ground (Figures 4d). The absence of liquid precipitation leads to results in better cooling in winter , and reduction of the and leads to a reduction in ALT thickness. Decreasing the Lower wind speed results in more efficient cooling for the full year (Figure 4a,b) as a result of changes in sensible heat fluxes over on the surface. The biggest effect occurs when the snow depth is reduced to zero greatest effect is seen when the natural isolating snow cover is absent (Figures 4e,f). This change results in a remarkable notable cooling of the ground in winter that supports the preservation of permafrost (Figure 4e)due to the removal of the natural insulation layer. This effect helps to cool permafrost during winter. . However, temperatures in the

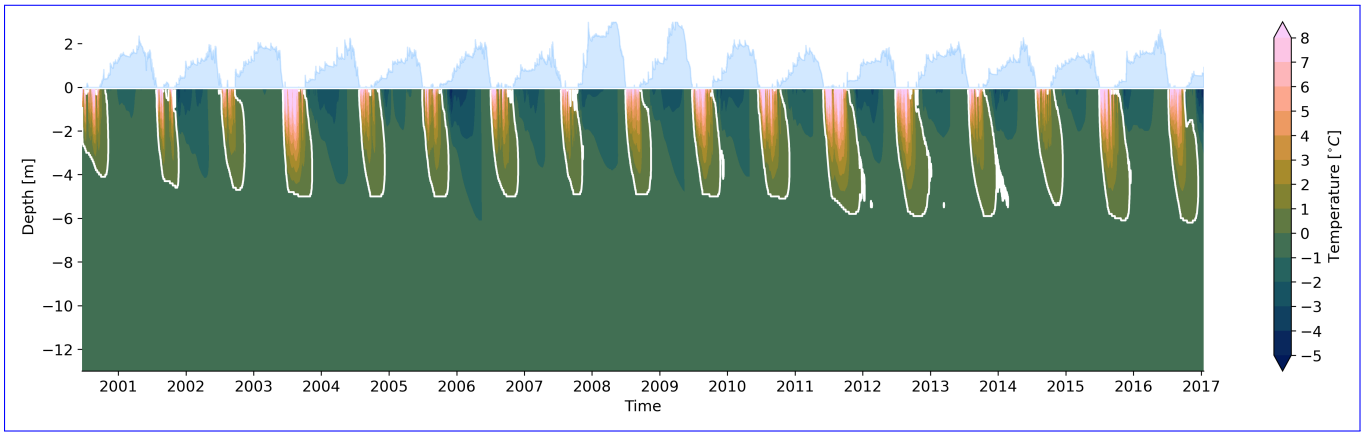

Figure 2. Time series of daily averaged modelled ground temperatures during natural undisturbed conditions at the Schilthorn site from 2000 to 2017. ~~Black~~ White contours indicate the 0 °C isotherm, i.e, the ALT. Snow depth is indicated in light blue above the 0 m depth level.~~The 0 °C isotherm is outlined as black contour.~~

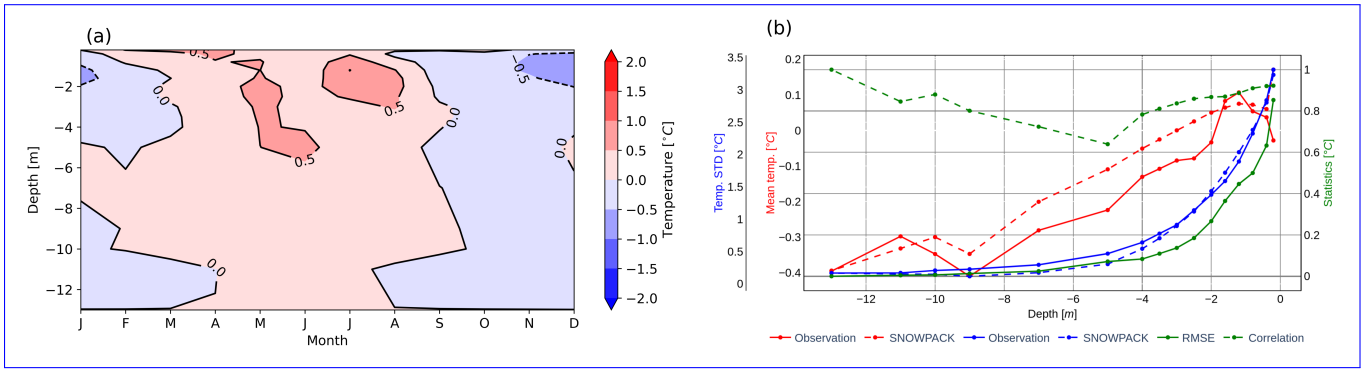

Figure 3. Comparison between modelled and measured ground temperatures at the Schilthorn site from 2000 to 2017. (a) Monthly averaged differences. Red (blue) colours indicate model temperature higher (lower) than observations. ~~The solid (dashed) black contour lines represent positive (negative) isotherms.~~ (b) Statistical analysis of the ground temperature differences averaged over the 17 years period. The 3 vertical axes ~~show~~represent: mean temperature (red), standard deviation (blue), other statistics (green). The horizontal axis indicates depth.

~~summer season increase since during the usual melting season the absence of snow is no longer protecting~~ summer increase because snow cover does not protect the ground from heat exposure and the favourable albedo effect is missing. If no snow is accumulated, the benefit of ~~the~~ natural insulation is lost and the warming of the ground starts earlier than otherwise (Figure 4f). ~~In that case, the lack of snow during the melting season affects negatively the ground temperatures, and the heat taken from the ground in~~ Heat loss during winter is not enough to compensate for the absence of snow. Finally, shading the ground from ~~the incoming~~ direct short-wave radiation (Figures 4g,h) results in ~~decreasing the temperatures of the ground ,~~ lower ground temperatures in winter and, especially, in the summer season. This occurs because the ~~energy received through radiation is not~~

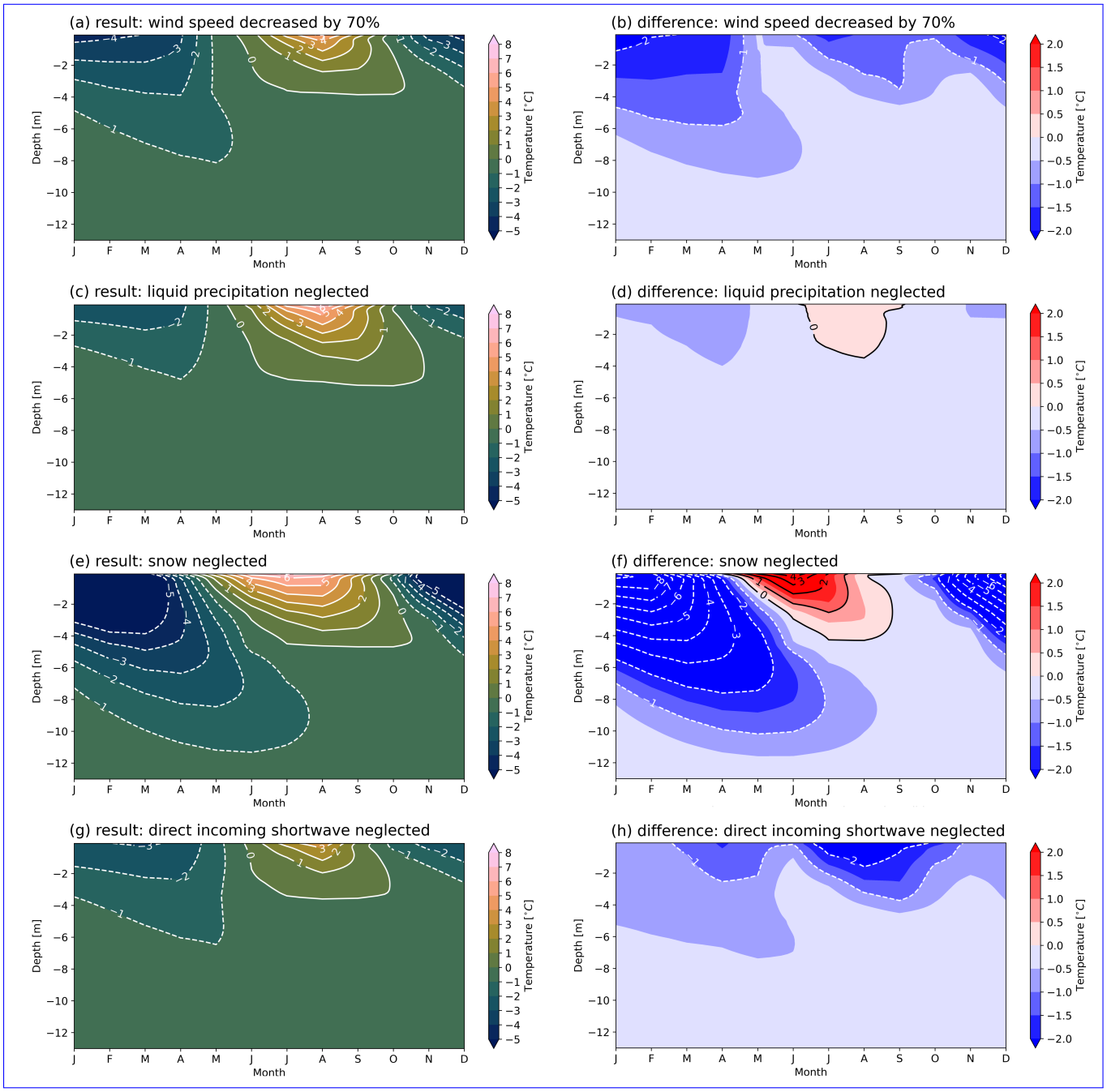

Figure 4. Monthly averaged modelled ground temperatures at the Schilthorn site from 2000 to 2017 resulting from individual model configurations defined in the ~~"~~'shading~~"~~' experiment (~~Section~~Exp. ~~4.2.1~~#2, Table 3). Panels (a, c, e, g): simulated ground temperature, panels (b, d, f, h): difference between simulated and natural conditions. Red (blue) colours indicate model temperature higher (lower) than observations. Experiments shown: (a, b) - wind speed reduced by 70% (Exp. #2.1); (c, d) - liquid precipitation set equal to zero (Exp. #2.2); (e, f) - snow depth set equal to zero (Exp. #2.3); (g, h) - direct component of incoming short-wave radiation neglected (Exp. #2.4).

~~penetrating~~ incident radiative energy does not reach the ground and, as a result, the ~~depth of the thawing layer~~ ALT (0 °C) is ~~less important~~smaller.

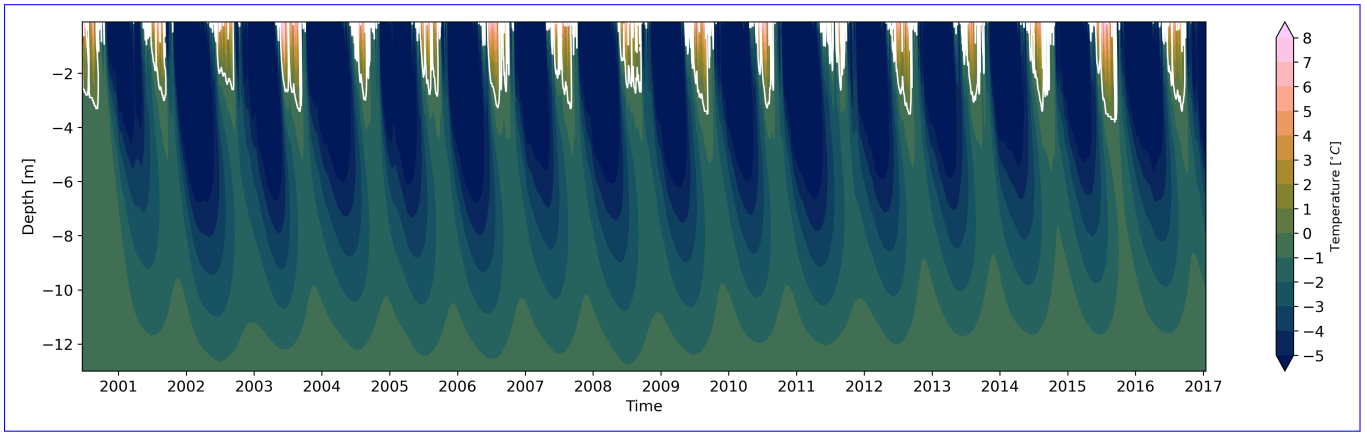

Figure 5. Time series of daily averaged modelled ground temperatures ~~from~~ presenting the net effect of the 'shading' experiment (Exp. #2.5, Table 3) at the Schilthorn site for the period of 2000 to 2017. ~~Black~~ White contours indicate the 0 °C isotherm, ~~i.e~~i.e., the ALT.

In Figure 5 the ~~total~~ net effect of shading at Schilthorn is shown, demonstrating that ~~the~~ shading leads to cooling of the ground during winter and ~~decreases the~~ a decrease in ALT (depicted as the 0 °C isotherm in both figures). ~~However, there are positive temperature differences in the summer season, which provokes ALT remain at certain meters depth during the evaluation time, indicating that this method of stabilisation~~ In agreement with the results by Quinton et al. (2011) testing different shading devices and observing the ground temperature decreasing with time, we also find a decreasing trend in ground temperature in our simulation results. However, there is still enough heat input to keep the ALT at a depth of several metres (Table D1). This indicates that this stabilisation method is insufficient and ~~should~~ needs to be supplemented by ~~another, as was mentioned by (Cheng, 2005) and (Loktionov et al., 2022). This method cannot stabilise the cold region below the surface. On the contrary, it~~ other elements described by Cheng (2005) and Loktionov et al. (2022). In contrast, the method amplifies the annual cycle of thawing and refreezing. In the long-term trend (Figure 5), the net effect of this method allows rapid ground cooling ~~in the winter every year~~every winter, however, it does not create and maintain a thermal barrier layer even after 16 years~~in application, and consequently, the atmospheric heat continues to affect the ground temperatures~~.

5.2.2 Thermal insulation

In Figure 6, the effect ~~from year-round~~ of an artificial thermal insulation layer throughout the year is shown, presenting the monthly ~~averaged~~ average evolution of the ground temperature profile of the Schilthorn borehole. We examine two cases with different thicknesses of the thermal insulation layer ~~thicknesses~~ of 50 mm and 100 mm. ~~While~~ Although the placement of an insulation layer of 50 mm does not completely prevent temperatures above 0 °C (Figure 6a) it decreases the ALT in summer~~(Figure 6b)~~. In addition, Figures 6b and B1 demonstrate that the placement of an ~~extra~~ artificial insulation layer

~~decreases the heat loss~~ (Exp. #3, Table 3) effectively decreases the loss of heat to the atmosphere in winter. The ~~heat flux distribution~~ distribution of heat flux in the permafrost remains preserved, due to the ~~heat flux limitation~~ limitation in heat flux at the surface (Figure B1). However, ~~on the long-term~~ in the long term, the combination of ~~the atmospheric heat flux together with the geothermal heat flux~~ atmospheric and geothermal heat fluxes will warm the permafrost. ~~Furthermore, the deployment~~ Consequently, installation of an insulation layer of 50 mm thickness at the surface is ~~still~~ insufficient to preserve the permafrost table, and the ALT still comprises several ~~meters~~ metres (Figure 6a, Table D1).

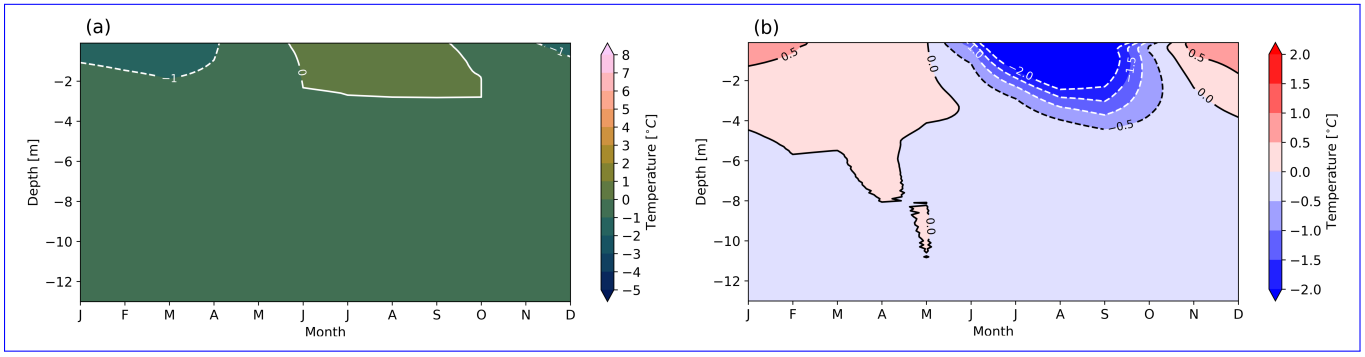

Figure 6. Modelled monthly averaged ground temperatures at the Schilthorn site for the period from 2000 to 2017 using a 50 mm artificial thermal insulation layer on top of the ground ~~all~~ throughout the year ~~round~~(Exp. #3, Table 3). (a) Temperature evolution in the ground. ~~Black contours indicate the 0 °C isotherm.~~ (b) Temperature difference compared to the undisturbed natural conditions. Red (blue) colours indicate model temperature higher (lower) than measurements.~~Solid (dashed) black contour lines represent positive (negative) isotherms.~~

~~Results~~ The results presented in Figure B2 show that the thicker the thermal insulation layer, the smaller its effect of thermal stabilisation. Instead of favouring ~~cooling of the ground~~ ground cooling during winter, ~~the~~ this artificial thermal insulation prevents the desired heat loss from the ground to the atmosphere. ~~Also~~In addition, it can be seen that decreasing the ~~insulation layer thickness allows for~~ thickness of the insulation layer allows some cooling in winter, but at the same time ~~, it~~ protects the ground less from heating in summer. The observed effects are plausible because snow accumulates ~~on top of~~ above the thermal insulation layer in winter, ~~lowering the natural heat loss~~ reducing the loss of heat from the ground. This suggests the existence of an optimal thermal insulation thickness. However, this optimum naturally depends on ~~the seasonal climatic conditions, as well as on~~ latitude, altitude, exposition, slope angle~~and local topography~~, local topography, and climatic conditions. Given the principal interest ~~of~~ in quantitatively assessing different engineering-based permafrost thermal stabilisation methods, we did not strive to determine this optimum for the Schilthorn site ~~, as we see this being out~~ and consider it outside of the scope of this study. The brief conclusion here is that the 50 mm thickness ~~provided the better contribution during both~~ yielded a better effect during summer and winter, compared to ~~the~~ cases with increased ~~thickness~~ (100 mm) and decreased ~~thickness~~ (10 mm~~, results not shown)~~) layer thickness. However, it ~~can be seen that also~~ also appears that this method is not efficient enough ~~for the long-term preservation of~~ to protect local alpine permafrost in the long term from the growing impact of atmospheric warming and increasing net energy input into the ground.

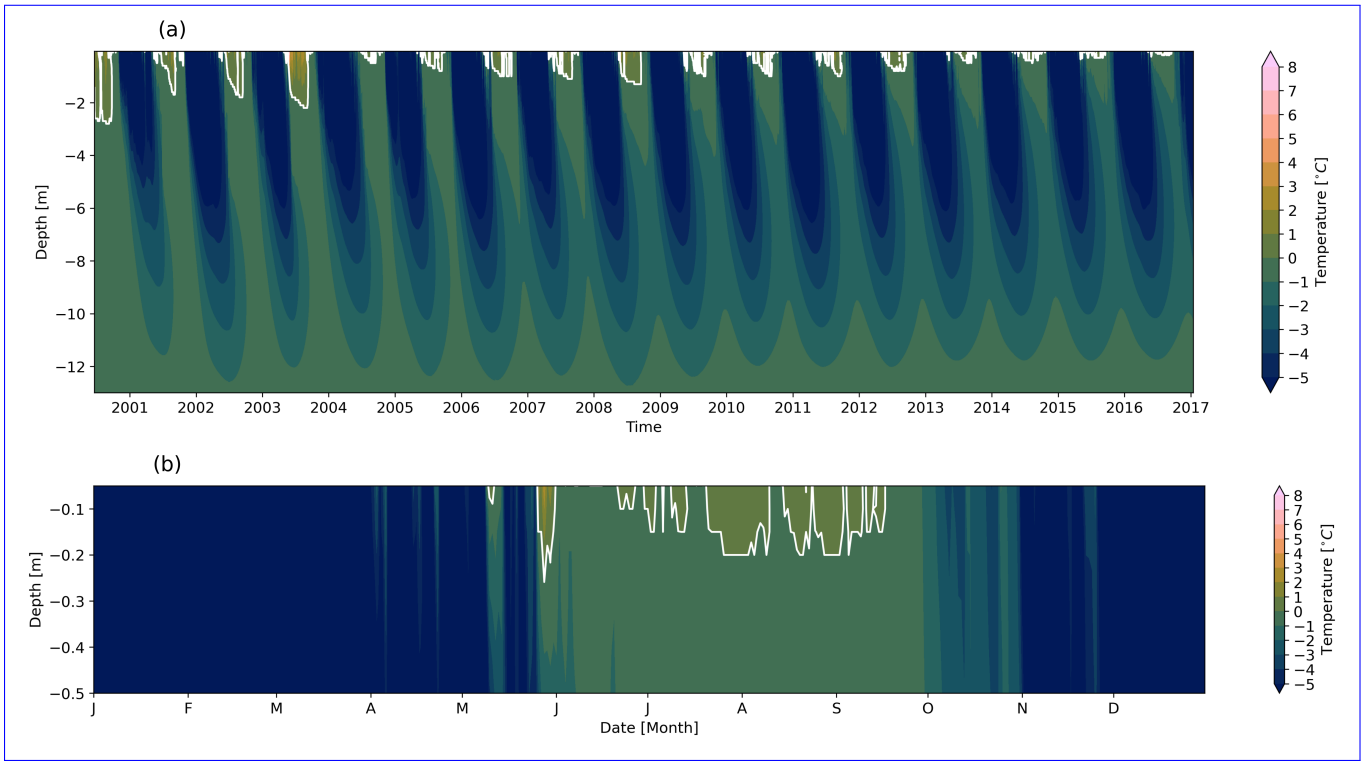

Figure 7. (a) Time series of daily averaged modelled ground temperatures from the heat transfer ~~regulation~~ attenuation experiment, (Exp. #4, Table 3) at the Schilthorn site for the period of 2000 to 2017. ~~Black~~ White contours indicate the 0 °C isotherm, i.e., the ALT. (b) Last year of the simulation, 2016, after 16 years of artificial thermal ~~ground~~ insulation of the ground.

~~As previously explained,~~ The timely placement/lifting of the insulation layer ~~can result in more~~ is the key to most effective cooling during ~~the winter season~~ winter and better preservation during ~~the summerseason~~summer. We examined the impact of heat transfer ~~regulation~~ control by combining the impact of thermal insulation with surface shading. Figure 7 shows that ~~with this approach the effect of cooling is intense in winter~~ this approach (Exp. #4, Table 3) results in intense winter cooling over a multi-year period while favouring heat loss ~~in~~ from the ground to a depth of about 10 m (Figure 7a). In this case, heat flux attenuation (Sharaborova and Loktionov, 2022) is sufficient for thermal stabilisation of the permafrost (Table D1) and is more efficient in cooling when installed on site than continuous thermal insulation (Luo et al., 2018). This method also results in a gradual decrease in ALT over the years, demonstrating that the winter cooling effect surpasses the ~~warming effect of summer . Additionally, the placement of~~ summer warming. In addition, thermal insulation during ~~summer helps~~ the summer helps to protect the permafrost by reducing ~~penetration~~ the transfer of heat from the atmosphere. Taking a closer look at the last year of the simulation (Figure 7b) reveals a temperature decrease in near-surface layers and ~~significant ALT reduction~~ a significant reduction in ALT with this approach. Figure B3 indicates the continuous ~~heat extraction during wintertime, explaining~~ loss of heat during winter, which explains the preservation of low ~~temperatures in the ground~~ ground temperatures. This cooling

mechanism can be sufficient for creating a thermal (cold) "barrier" layer near the surface to protect the ground ~~beneath over an entire~~ underneath over a whole year (Figure 7). Although the creation of a "barrier" layer takes ~~many~~ several years in the simulation, with unstable conditions occurring during its formation, after 16 years the ALT was decreased ~~by~~ to several decimetres. We expect this method ~~might~~ to be even more effective ~~and used with more benefits~~ when used in combination with active cooling since it creates an additional "shield" of thermal insulation ~~, which will help to preserve the actively applied cooling at depth while decreasing the~~ and further decreases heat exchange with the atmosphere.

5.2.3 Thermal stabilisation with active cooling

~~We examine now~~

We now examine the effect of the proposed thermal stabilisation system with active cooling (Section 4.2.3)~~)~~, first quantifying the effect ~~from~~ of the cooling pipes alone ~~and second the total~~ (Exp. #5, Table 3) and then the combined effect of the system ~~including the solar panels shading the ground.~~ that includes shading of the ground from the solar panels (Exp. #6, Table 3). We examine the distribution of temperature and heat flux ~~distribution~~ in the ground to observe ~~if~~ whether a thermal barrier layer is ~~created.~~ developing.

Figure 8 shows that when ~~the active cooling system is in operation,~~ active cooling is applied (Exp. #5, Table 3), sub-zero temperatures of the permafrost ~~stabilise~~ establish after 4 years ~~of application of the cooling method~~ with temperatures well below 0 °C at depth. The ~~top~~ upper layers of the last simulated year (Figure 8b) show that the thawing boundary, indicated by the 0 °C contour, does not extend deeper than ~~40 cm . This demonstrates~~ 25 cm demonstrating the effectiveness of the cooling method in creating a thermal barrier layer and limiting heat ~~penetration~~ transfer during summer.

The ~~heat flux distribution~~ distribution of heat flux shown in Figure 9 (Exp. #5, Table 3) illustrates the consequences of the formation of a thermal barrier layer. The large heat fluxes in the upper layers are due to the strong temperature gradient between the ~~air temperature~~ ground surface and the cooling pipes, the latter conserving a constant low temperature around them. This determines the direction of the heat flux ~~downwards~~ downward from the surface to the level of the pipes. In depth, the heat flux ~~has the opposite sign. Combined~~is directed upward toward the pipes. Together, these heat fluxes indicate ~~heat extraction~~ the extraction of heat from the ground ~~via~~ through the cooling liquid that circulates in the pipes~~, demonstrating the positive effect of the cooling.~~ .

Figure 8a shows that after the establishment of the barrier layer (after about 4 years), the soil cools ~~down below~~ to a level of ~~about~~ approximately 3 m, which may be related to the ~~given structural ground stratigraphy~~ structural stratigraphy of the ground given (Table 2). ~~The reason why the formation the stable barrier layer~~ Due to thermal inertia and slow heat conduction in the ground, it takes several years ~~, is that it take time to establish the energy balance in the ground~~ to form a stable thermal barrier layer (Figure 8). ~~This balance is established when the~~ Once enough heat is ~~extracted~~ lost from the ground, ~~and when the purpose of the system is switching~~ the system switches from cooling to keeping the in-depth temperatures stable ~~along~~ in the following years. Due to the temperature boundary conditions at the bottom ~~used in the model (see~~ of the model domain (Section 4.1 the model ~~strives to establish the energy balance between layers, and when equilibrium is reached the heat exchange between layers~~

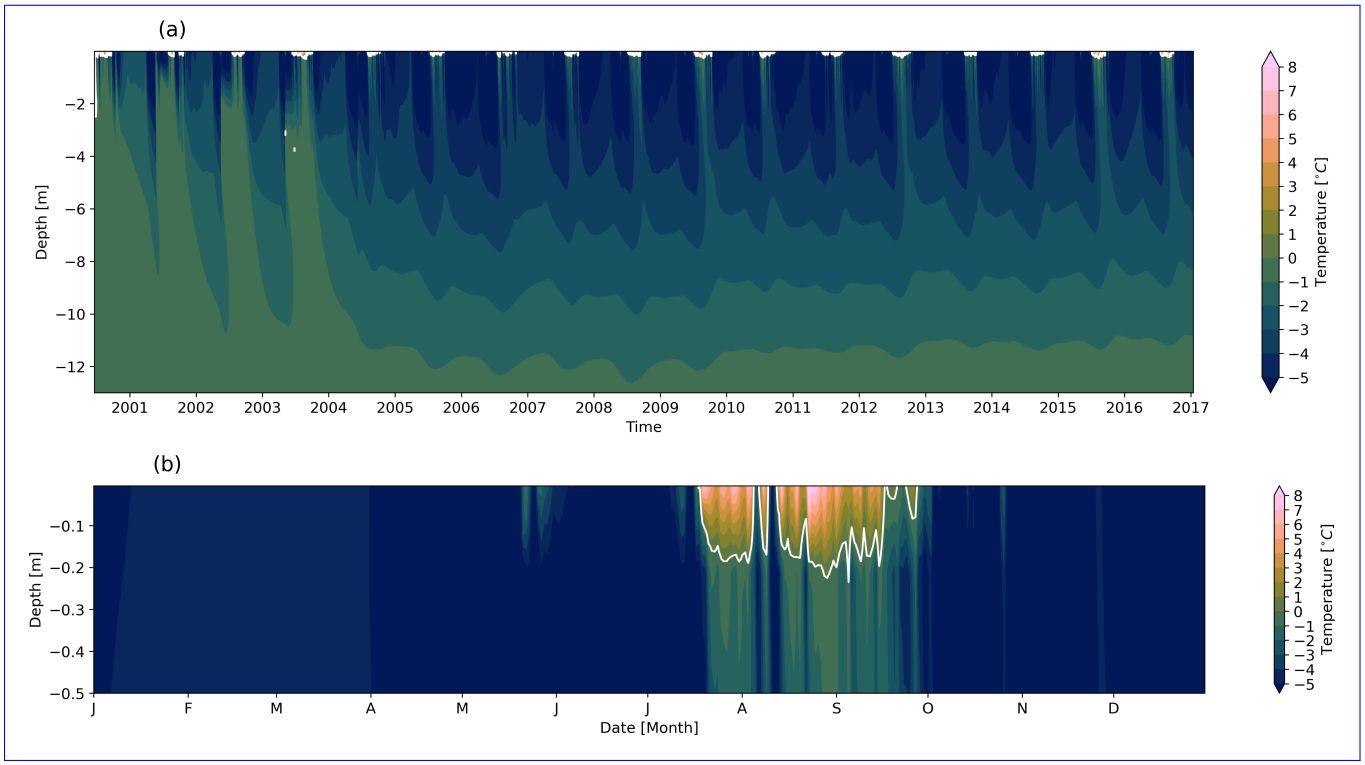

Figure 8. (a) Time series of daily averaged modelled ground temperatures from the cooling pipes experiment (Exp. #5, Table 3) at the Schilthorn site for the period of 2000 to 2017. ~~Black~~ White contours indicate the 0 °C isotherm, i.e., the ALT. (b) Last year of the simulation, 2016, after 16 years of active cooling.

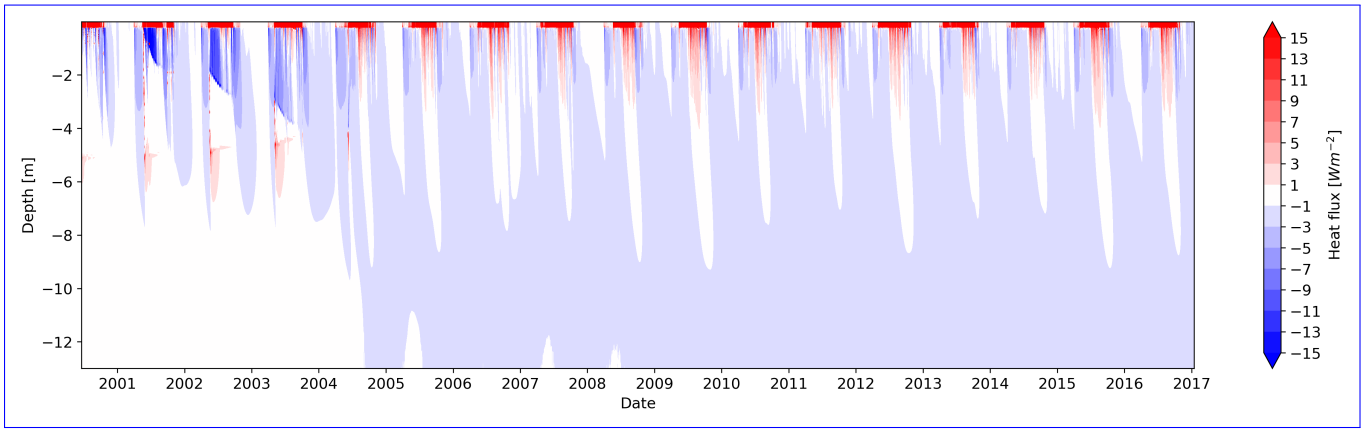

Figure 9. Time series of daily averaged modelled conductive heat flux from the cooling pipes experiment (Exp. #5, Table 3) at the Schilthorn site for the period of 2000 to 2017.

~~is aimed at maintaining this balance~~ evolves toward a steady state (Figure 9). ~~This case with only active cooling, demonstrates well the reaction of the ground to external active cooling.~~

~~After demonstrating the cooling effect of the pipe system alone, we~~ We now focus on the full system ~~combining~~ that combines active and passive cooling methods, i.e., ~~the ground~~ including shading with the solar panels ~~. Simulation~~ (Exp. #6, Table 3). The simulation results presented in Figure 10 show that this combined effect is favourable for the ~~conservation~~ preservation of permafrost due to the formation of a more pronounced sub-freezing thermal barrier layer compared to ~~results from~~ the results of both systems independently. The effect is also more immediate and does not ~~require several years for establishing~~ take several years to establish the thermal barrier layer (Figure 10a). In the ~~final~~ last year of the simulation (Figure 10b), it is evident that the impact of summer warming cannot be fully suppressed or compensated for. However, the engineered cooling method significantly reduces the ALT compared to natural conditions, achieving a difference of several ~~meters.~~ metres. Our results show that the combination of active and passive cooling is sufficient to stabilise not only the continuous permafrost of the lowlands, as shown by Loktionov et al. (2022), but also the mountain permafrost (Table D1).

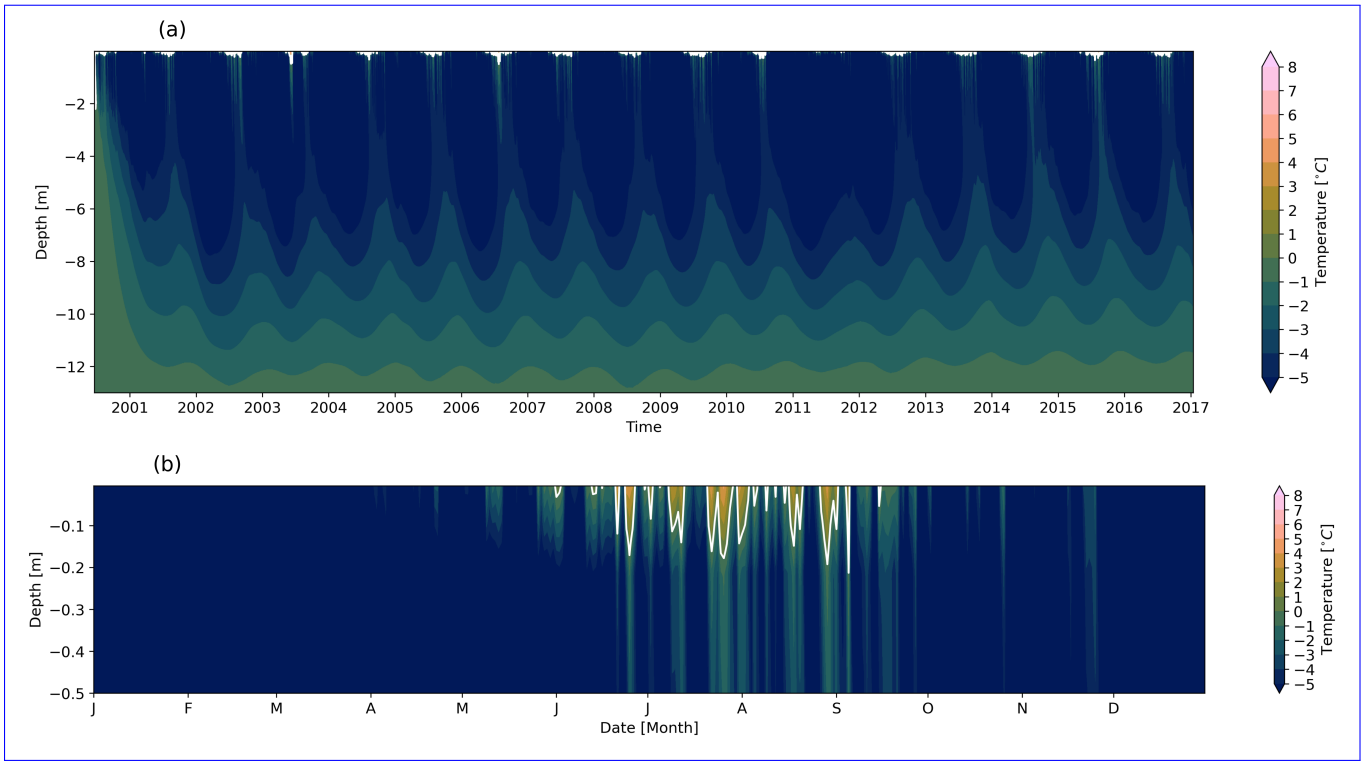

Figure 10. (a) Time series of daily averaged modelled ground temperatures from the experiment combining cooling pipes and solar panel shading (Exp. #6, Table 3) at the Schilthorn site for the period of 2000 to 2017. ~~Black~~ White contours indicate the 0 °C isotherm, i.e., the ALT. (b) Last year of the simulation, 2016, after 16 years of active cooling and shading.

The evolution of the conductive heat flux ~~evolution instigated~~ initiated by the combined cooling system (Exp. #6, Table 3)(Figure 11) shows that in addition to the effect ~~from cooling pipesdescribed before, the~~ of the cooling pipes, passive cooling works ~~in~~ during the winter season. This corresponds to the heat evacuation from the depth in winter, when the heat flux direction is upwards (Figure 11a). Figure 11b indicates that the highest heat flux values occur in the layer between the surface and the pipes from April to the end of October, when ~~the~~ active cooling is applied. This downward heat flux extends to ~~about 10 cm below~~ the cooling pipes, which arises as a result of the strongest temperature gradient. ~~Beneath~~ Below this level, the heat flux ~~decreases eventually approaching~~ eventually decreases to 0 ~~Wm^{-2}~~ Wm^{-2}. In winter, heat is lost to the cold atmosphere~~turning the sign of the~~ , turning the direction of heat conduction. Figure C1 presents the daily heat flux and temperature profiles, illustrating the evolution of conductive heat flux and ground temperatures over time and highlighting their dynamic behaviour throughout the simulation.

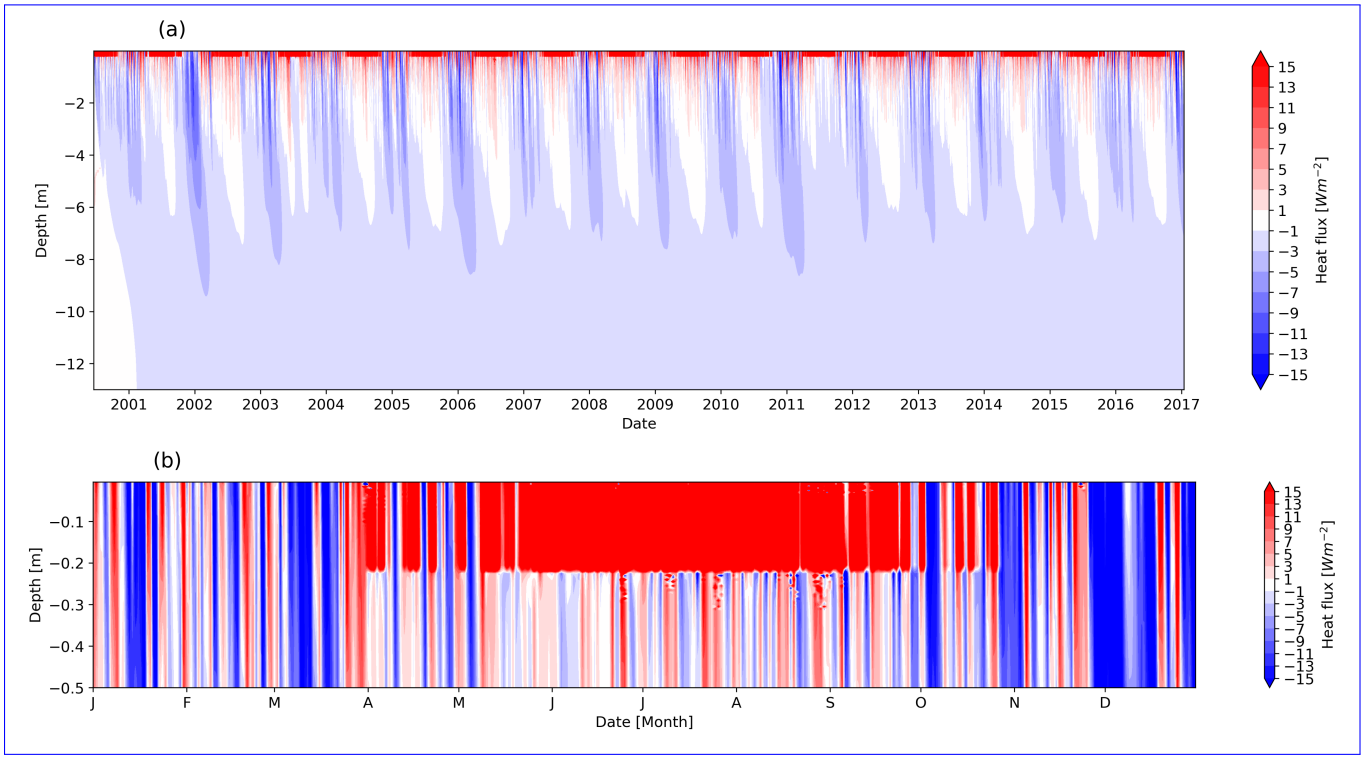

Figure 11. Time series of daily averaged modelled conductive heat flux from the experiment combining cooling pipes and solar panel shading (Exp. #6, Table 3) at the Schilthorn site for the period of 2000 to 2017. (b) Last year of the simulation, 2016, after 16 years of active cooling and shading.

5.3 Analysis and discussion of stabilisation effects

~~For the considered mountain regions~~

For the mountain regions considered, the most efficient method of thermal stabilisation was active cooling combined with effects from passive methods such as surface shading with solar panels. In the experiments ~~in~~ described so far (Section 5.2.3~~all solar radiation was used for powering~~) all the photovoltaic energy produced was used to power the heat pump. ~~Despite the fact that the~~ The main objective is to set as much energy as needed for ~~the coolingpurpose~~cooling. However, we also tested the case ~~, when~~ where only a partial amount of ~~available energy from the solar panels~~ the available PV energy is reserved for ~~the coolingpurpose~~cooling. This case may ~~bring~~ serve as a more realistic and practical demonstration of the system application, as it could imply the potential ~~for using~~ to use smaller panels or other ~~optimizations~~ optimisations in system design. It allows ~~to challenge~~ for challenging the system, in case ~~when~~ the surface for installation is limited and the energy should be redistributed between ~~the cooling and~~ cooling and other infrastructure energy supply. We show a situation in which only 50% of the incident solar radiation is used ~~for powering~~ to power the heat pump, i.e., for cooling ~~,~~ (Exp. #7, Table 3), reserving the other half for the power grid or other needs in the vicinity of the site. ~~As it was explained in methods (Section 4.2.3), the surface that is cooled is equal to the surface of solar panels~~Recall that the cooled surface has the same area as that of the solar panels (Section 4.2.3). In the following part~~we made~~ , we perform some experimental tests, ~~with~~ cutting the energy supply directed to cooling by a certain amount, to look at the ~~robustness~~ resilience of the system in different ~~combination~~configurations.

In the case where only half of the generated PV energy is used for cooling (Exp. #7, Figure 12), we applied cooling ~~the entire year, unlike~~ in summer, similarly to the case discussed in Section 5.2.3 Exp. #6, where cooling occurs ~~only~~ from April to October. This energy ~~partitioning~~ partition between cooling and the grid aims to maintain the same ~~persistence and temperature~~ temperature and persistence of the barrier layer as in Exp. #6 (Figure 10). However, ~~it can be seen that~~ with half the amount of ~~power~~ cooling power, the barrier layer is not as stable as with the 100% energy supply. ~~The ALT is increased~~ In addition, the ALT increases when using less power (Figure 12b) compared to the case ~~when using~~ applying 100% ~~energy for cooling~~ (Figure 10b). Recall ~~,~~ that the creation of an efficient barrier layer only with cooling pipes requires 5 full seasons with 100% power supply, applying cooling from April to October. It can be ~~noted that~~seen that, due to the initial ~~spin-up process to create~~ adjustment process creating the thermal barrier layer, ~~initially most~~ most of the PV energy is ~~used for cooling~~ initially used to cool the system. Once the barrier layer is ~~temporally stable and established~~ established and stable in time, a larger fraction of the produced PV energy can be injected into the grid. However, it is worth acknowledging that active cooling may not necessarily need to bring the system to a new equilibrium, and maintaining the existing thermal balance might be sufficient. It should be noted that our results did not explicitly test this~~, ~~; we assumed a simplified case ~~where~~ in which the energy is evenly split between cooling and grid injection. In a ~~real applicationcase~~real-world application, the system control will become completely dynamic, ~~i.e., which is considered to be the~~ an ultimate goal of the system application. ~~It is important to give priority to cooling when required, otherwise~~ Priority should be given to cooling before feeding into the grid. For the design of a suitable PV system, it is therefore imperative to know the energy demand for the creation and maintenance of a thermal barrier layer in alpine permafrost, which can be ~~available from simulations~~ obtained from numerical simulations, as demonstrated in the previous sections. The optimal choice will enable reliable cooling of the ground while bearing the potential of providing significant excess power to the grid or nearby installation, especially after the initial ~~ramp up~~ ramp-up time.

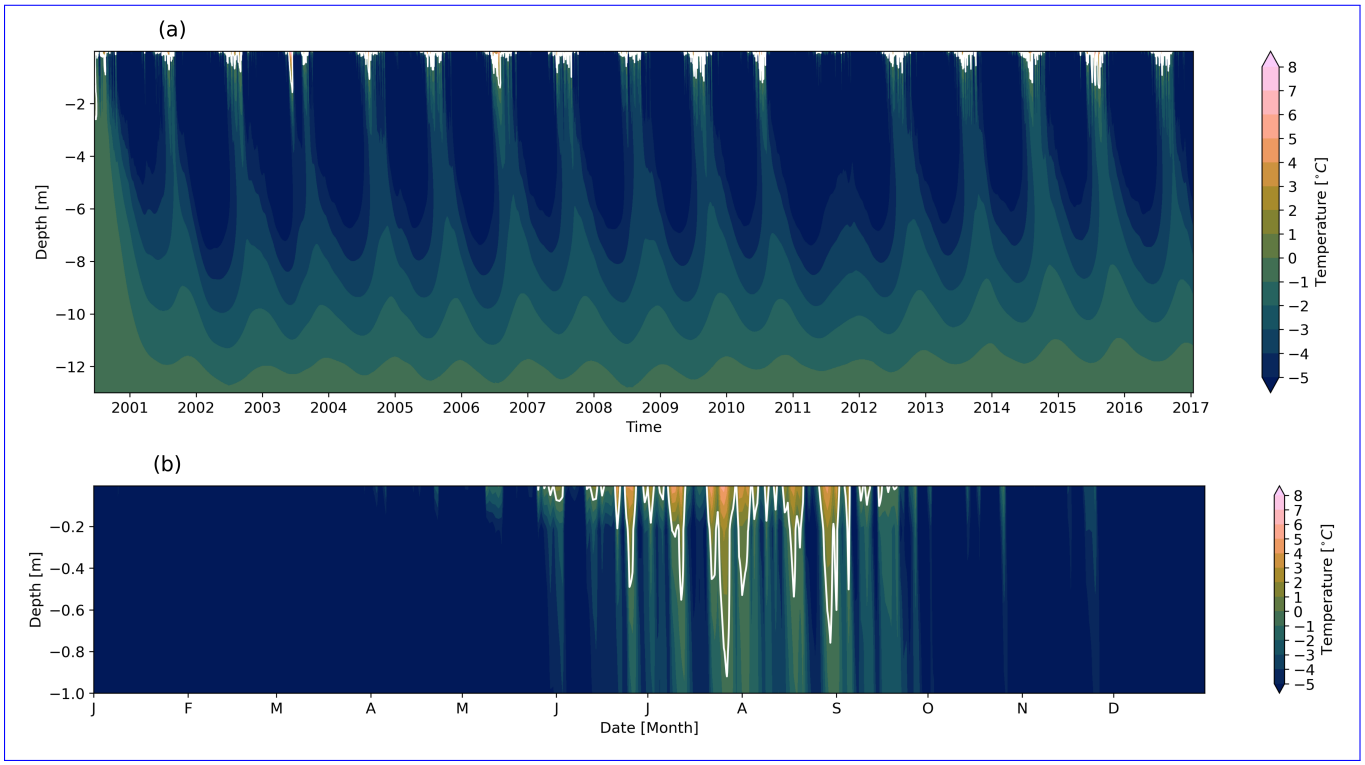

Figure 12. (a) Time series of daily averaged modelled ground temperatures from the experiment combining cooling pipes and solar panel shading but using only 50% of available energy for cooling (Exp. #7, Table 3) at the Schilthorn site for the period of 2000 to 2017. ~~Black~~ White contours indicate the 0 °C isotherm, i.e., the ALT. (b) Last year of the simulation, 2016, after 16 years of active cooling and shading.

Another alternative is the combination of active cooling (~~Section 4.2.3~~Exp. #6, Table 3) with heat flux ~~regulation (Section 4.2.2~~attenuation (Exp. #4, Table 3) as discussed in Section 5.2.2 and presented in Figure 7, when during summer the ground was also protected with thermal insulation material. In that case, ~~there is no need~~ it is not necessary to wait until the snow has melted to lay out the thermal insulation as discussed in Section 5.2.2, however, it is important ~~for the heat flux regulation to follow the active cooling implementation. When~~ that the application of thermal insulation to attenuate heat flux is coordinated with the period of active cooling. During the active cooling ~~is applied (from~~ period (April to October)~~the~~ , thermal insulation is placed on the ground ~~, and when the active cooling is deactivated the thermal insulation should be lifted. This combination helps better conserve the low temperature created by the cooling pipes in the ground during summer, and in winter it allows for the natural cooling process~~and removed when it is deactivated to allow effective winter cooling. This setup improves the efficiency of the cooling system by preserving low ground temperatures in summer while allowing natural cooling in winter. In this case, a ~~thermal insulation material of~~ 50 mm ~~thickness is used, which was numerically tested here and~~ thick thermal insulation is simulated and was found to be ~~the most efficient . The use of combination of different methods, the active coolingwith shading~~efficient protection. The combination of active cooling, shading, and heat flux ~~regulation, helps to entirely achieve the stabilization~~

attenuation leads to the desired stabilisation effect. It allows us to use less ~~energy from solar panels~~ PV energy for cooling and send more to the grid even in ~~case when~~ the case where the cooled surface area is equivalent to the surface of ~~solar panels~~the solar panels used. As in ~~the experiments explained above we tested the~~ experiments #7-#8, we tested different cases when only ~~the~~ a certain amount of ~~energy is led to~~ the available PV power is used for cooling. Here~~due to~~ , due to the effective preservation of cold in the ground established by heat flux ~~regulation~~attenuation, we found ~~that in this specific case for the modelled site , the case of the active cooling in combination~~ for our test site that when combining active cooling with heat flux ~~regulation~~ attenuation the energy required for cooling can be ~~reduced to~~ as low as 10% of the ~~one taken from the solar panels.~~produced PV power (Exp. #8, Table 3).

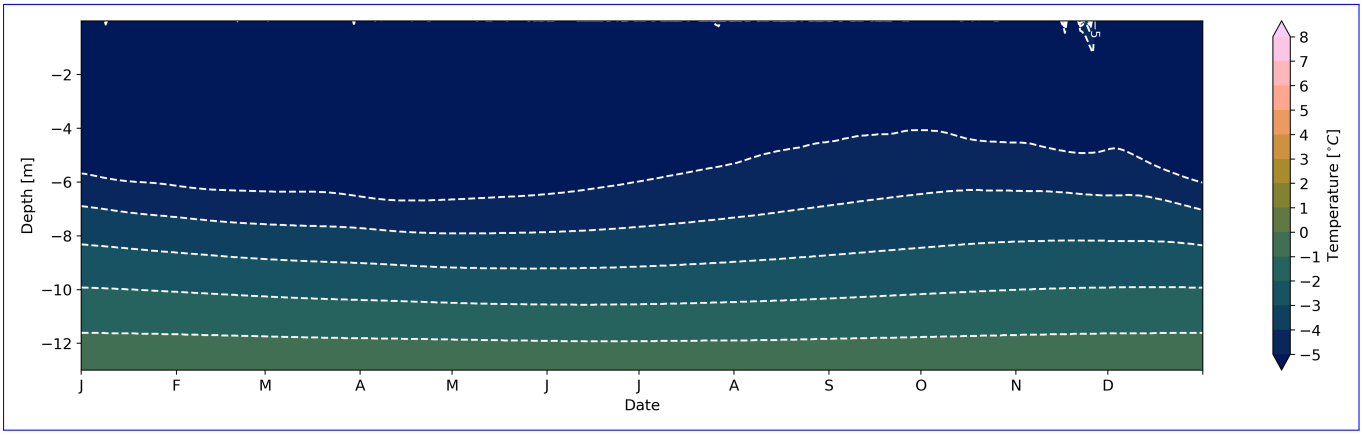

Figure 13. Daily averaged modelled temperature from the experiment combining heat flux attenuation by thermal insulation with active cooling ~~pipes~~ and ~~solar panel~~ shading ~~but~~ using only 10% of ~~available energy~~ the produced PV power for cooling (Exp. #8, Table 3) at the Schilthorn showing the last year of the simulation, 2016, after 16 years of active ~~cooling~~ and ~~shading~~passive cooling.

As ~~the~~ visible in Figure 13~~shows~~ , the conservation of the cold temperature resulting from ~~heat flux regulation with thermal insulation ,~~ thermal insulation helps to keep the ALT ~~as shallowas possible. This brings the better~~ shallow. This results in more efficient cooling and heat ~~extraction~~ loss from the ground ~~comparing to the~~ compared to cases of active cooling ~~only~~ alone (Figure 8), or active cooling with shading (Figure 10). Another positive aspect of this combined method is that ~~it ensures not all produced PV energy is spent on~~ not all the PV power produced is used for cooling only, as ~~it was in the case demonstrated in~~ was the case in Exp. #6 (Figure 10~~. As previously discussed, limiting~~). Limiting the energy used for cooling without ~~regulating~~ modifying the natural conductive heat flux is possible ~~and~~ but recommended to be 50% or higher; otherwise, the active layer will remain deep. When combined with heat flux ~~regulation~~attenuation, this approach offers greater flexibility in managing the power received from solar panels. We also suggest that intense and continuous cooling might be unnecessary~~,~~ ; it can be adjusted based on the monitored state of the permafrost, its temperatures, and also ~~based on the~~ on atmospheric conditions. The latter determine which combinations of the stabilisation systems should be applied in different climatic conditions. Although site-specific decisions require local calibration, our simulations provide a basis for such adaptive strategies. The simulated ALT results are presented in Table D1 for a better overview and comparison.

6 Conclusions and outlook

Permafrost thawing causes severe problems such as infrastructure damage or destruction, rock falls, land slides, and other environmental disasters. This study uses numerical simulations to investigate the effect of different engineered mitigation strategies targeted at thermally stabilising permafrost through various passive and active cooling methods. All these methods are geared to artificially cool the ground, limit or favour heat exchange with the atmosphere depending on the season, preserve the permafrost, and minimise the seasonal ALT. One of these methods consists of technically creating and maintaining a cold thermal barrier layer that protects the permafrost underneath from heat conducted from the surface into the ground, particularly during summer when solar radiation input is large. The energy required for the technical cooling of the ground is obtained from installations of collocated solar panels, which are also creating favourable shading of the ground.

A series of numerical experiments assesses several technical solutions or combinations of such thermal stabilisation systems, to demonstrate and quantify their efficiency when applied in alpine permafrost. For the simulations, We use the 1D SNOWPACK model (Section 2) for reproducing the mountain permafrost at a representative alpine location, the Schilthorn site, canton Bern, Switzerland, (Section 3). This site features a time series of observational borehole data for comparison and validation of the model simulations. A first simulation reproduces the natural undisturbed conditions at the Schilthorn site (Section 4.1) configuring the model with parameters of the local substrate measured at that site (Section 5.1). Then, different thermal stabilisation methods were implemented numerically (Section 4.2), to show their ability in cooling the ground and keeping it preserved. Both passive, active, and combined thermal stabilisation systems were tested and their efficiency assessed (Sections 5.2, 5.3). Simulation results indicate that different combinations of thermal stabilisation systems are able to produce the successful effect and to cool the ground sufficiently. However, their efficiency varies depending on the methodology applied.

The tests of passive thermal stabilisation with shading of the surface (Section 4.2.1) do not show the desired long-term effect for thermal stabilisation. It has a good effect during winter, due to natural cooling, however, in summer the ALT stays almost unchanged compared to the natural conditions (Section 5.2.1). Another passive cooling system consists of a thermal insulation layer on top of the ground (Section 4.2.2). In this experiment, two configurations are tested: (a) year-round covering the ground with insulation material and (b) deploying and lifting of the insulation layer depending on the season. The year-round configuration does not result in significant thermal stabilisation, while the season-dependent deployment and removal of a thermal insulation layer effectively regulates the conductive heat flux at the ground surface leading to favourable stabilisation effects (Section 5.2.2). Seasonal heat flux regulation method of thermal stabilization significantly reduces the ALT, although it requires several years to fully achieve this effect.

The active cooling system using pipes in the ground (Section 4.2.3) is able to create a stable continuous thermal barrier layer but only after a 4-years spin-up period (Section 5.2.3). The best efficiency of a thermal stabilisation system is reached by combining active and passive methods (Section 5.2.3), which decreases the ALT to only a few tens of centimetres, and results in a stable barrier layer already after the first year. Thus, it is concluded, that the best cooling efficiency is achieved by a tailored combination of active and passive methods. The combination of active cooling, shading, and the heat flux regulation with the temporary thermal insulation layer which reduces warming and favours cooling has the strongest effect (Section 5.3).

Knowing the amount of energy required for cooling~~and for~~ , creating and maintaining an effective thermal barrier layer to stabilise the underlying permafrost allows ~~for~~ optimal system design and power regulation. ~~Simulation~~ Simulations have shown that ~~for an optimal stabilisation system~~ only a fraction of the produced PV energy (50% for ~~only active cooling~~ active cooling alone and 10% ~~when active cooling is~~ for active cooling combined with heat flux ~~regulation~~attenuation) is necessary for ~~the~~ direct cooling of the ground. The excess energy is then available for the grid. ~~It is recommended that the applied stabilisation system dynamically regulates the required power supply for ground cooling~~ In an advanced application, the stabilisation system could be dynamically regulated depending on the monitored state ~~and conditions~~ of the permafrost~~(Sections 5.2 and 5.3)~~. However, ~~the convincing~~ optimal performance of the combination of active and passive cooling is difficult to achieve in the field ~~owing to~~ due to local climate effects and complicated installation in complex alpine permafrost terrain. In such cases, the use of a system similar to ~~(Loktionov et al., 2024b)~~ Loktionov et al. (2024b) could be an alternative, cooling ~~portions~~ parts of constructions directly with cooling pipes attached to basement walls, taking advantage of unused space in the foundation of a building and avoiding the installation of cooling pipes on inaccessible surfaces such as bedrock.

~~For a detailed assessment of the thermal stabilisation effects, it is essential to dispose of data of atmospheric conditions such as air temperature, solar radiation, wind speed, phase and quantity of precipitation, and snow depth from nearby meteorological stations or directly from sensors on-site. This enables a better understanding of the impact of passive thermal stabilisation Section 4.2.1 and Section 5.2.1. Due to the nature of simplified and idealised 1D simulations, i.e., the panels completely protect the ground from the snow and precipitation, not considering the possibility of lateral blowing snow, or leaking liquid precipitation through the gaps of adjacent solar panels Section 5.2,~~ Despite the efficiency of the ~~applied coefficient for wind speed decrease is empirical and its realistic value requires more advanced estimation. In-situ experimental field tests will further advance the study and understanding of the physical processes resulting from passive cooling due to the shading by the solar panels, and to better quantify the impact of this method.~~

~~Further refinement of the system is needed for an optimal choice of system variables such as depth and spacing of the cooling pipes , thickness of a thermal insulation layer, and the most efficient and economic way of creating and maintaining a thermal barrier layer while tuning the power regulation to dynamically adapt to real-time thermal permafrost conditions. The geometrical configuration of the cooling pipes in the ground needs to be adjusted to the local geo-cryological conditions for sufficient and most efficient ground cooling. Owing to the 1D simulations, such 3D effects could not be investigated in the present study. However, aspects as pipe spacing, diameter,~~ cooling system and its ability to create a thermal barrier layer, additional aspects must be taken into account, for instance, the topography of the terrain, water in the ground and associated heave, and difficulties linked with building in mountain permafrost that may cause some risks to infrastructure and the cooling system itself. One of the dangers is moisture present in the substrate during active cooling (Section 5.2.3) which can lead to heave and potential destruction of cooling pipes and ~~geometrical layout need to be adjusted to the conditions of the site to ensure optimal cooling as well as maximum solar energy yield at the given site and geographical region. Optimal system regulations is required for most efficient cooling and for protecting infrastructure at risk.~~ solar panels and cause damage to nearby structures. That is why for specific applications the simulated case must be adapted according to local ground properties and moisture conditions, the existing ground temperature distribution, ground-atmosphere heat exchange, topography, exposition, local

climate, and potentially existing construction characteristics. It remains a challenge to apply a thermal stabilisation system in alpine permafrost without altering the structure and mechanical processes in the ground.

Up-scaling the system to larger cooling areas is another direction of research. ~~At this stage, the numerical modelling~~ The presented numerical modelling framework could be extended to other permafrost types~~(continuous –~~, e.g. continuous (Arctic and Polar ~~zones; discontinuous - Subarctic zone), which will also allow~~ regions) and discontinuous (Subarctic regions), to investigate the performance of thermal stabilisation systems in different climatic regions and to propose an optimal combination of system components for ~~different~~ these conditions. The present study constitutes a detailed and systematic numerical investigation ~~for~~ of the choice and performance of permafrost stabilisation methods. ~~Results~~ The results are intended for the design and implementation of prototype installations and for up-scaling to real-world applications. The forthcoming challenges involve conducting experimental tests to validate the hypothesis, evaluating the influence of climate change on permafrost dynamics both with and without stabilisation measures, and devising an optimised methodology for thermal stabilisation tailored to diverse sites and climate conditions.

~~Despite the efficiency of the cooling system and the resulting successful creation of a barrier layer creating, it is important to note that a few additional aspects which are not considered here have to be taken into account, for instance, the terrain topography, and potential difficulties of building on mountain permafrost. These together with other natural hazard factors may bring up some risks for the infrastructure and cooling systemitself. One of the dangers is linked with active cooling and moisture present in the substrate (Section 5.2.3). Intense cooling bears the risk of ice formation in wet ground, which may lead to heave and potential destruction of solar panels and~~

5.4 Model assumptions and limitations

In the following, we consider the limitations of the modelling framework and the implications of key assumptions that may influence the findings.

Due to the nature of simplified and idealised 1D simulations, that is, solar panels completely protect the ground without gaps between adjacent panels from snow and precipitation, no lateral snow drift, and the applied coefficient for wind speed decrease is empirical and its realistic value requires more advanced estimation (Sections 5.2.1 and 5.2). In addition, the use of one-dimensional simulations limits the investigation of three-dimensional effects such as subsurface lateral heat flow and complex geometric configurations of infrastructure. This simplification may not fully capture interactions present in real-world applications, particularly when optimising cooling pipe layouts under heterogeneous geo-cryologic conditions.

Another limitation of the 1D formulation is the representation of the pipe cooling system. The model prescribes a constant temperature in the pipe, not considering the fluid temperature difference at the entrance and exit of the pipe due to heat exchange with the surrounding ground, as would be the case in a 3D situation. Another approximation is that the calculation of the power required for cooling is simplified and is effective only in the presence of solar radiation. The current state of the model allows us to assess the thermal stabilisation potential of a system and show its effects when applied at a permafrost site. However, for a real-world application, a full 3D model and a real-time monitoring system should be used to dynamically adapt the necessary cooling power supply according to the conditions of the permafrost and the solar power production. In addition,

further refinement of the system is needed for an optimal choice of system variables such as the depth and spacing of the cooling pipes, ~~and damages to nearby constructions which are supposed to be protected. That is why for specific applications the simulated case must be adapted according~~ the thickness of a thermal insulation layer, and the most efficient and economic way to create and maintain a thermal barrier layer while regulating power to dynamically adapt to real-time permafrost conditions and ALT. The geometric configuration of the cooling pipes in the ground needs to be adjusted to the local ~~ground properties and moisture conditions ,~~ geo-cryologic, topographic, and climatic conditions for sufficient and most efficient ground cooling.

The simulation framework employs a bucket water scheme, which has inherent limitations in representing soil water retention and redistribution. Although more detailed approaches such as the Richards equation could capture capillary-driven and preferential flow, these rely on assumptions that may not hold in coarse, rocky permafrost soils where voids and cracks dominate and capillary action is minimal. Therefore, it is uncertain whether the Richards equation would offer improved accuracy in such terrain. Additionally, given the slope of the terrain at the site, percolating water may not only seep vertically but also laterally, which is not accounted for in the ~~existing ground temperature distribution, ground-atmosphere heat exchange, topography, exposition, local climate, and potentially existing construction characteristics. It remains a challenge to apply a thermal stabilisation system in alpine permafrost without altering the structure and mechanical processes in the ground~~current model. More relevant is probably considering slope flow and water percolation in a 3D version of the model.

~~This study shows an example of~~ Additionally, although SNOWPACK includes evaporation, its interaction with the bucket scheme simplifies the representation of latent heat exchange. In this model, only the surface layer contributes to evaporation, and once it dries out, evaporation ceases. This limits the model's ability to simulate continuous moisture-driven cooling via latent heat fluxes.

6 Conclusions

Thawing permafrost triggers hazards such as structural damage, rockfalls, and landslides, which increasingly threaten the ~~implications faced by infrastructure built on the mountain permafrost. With permafrost temperatures rising, the~~ stability of ~~infrastructure is increasingly at risk (Duvillard et al., 2021). Currently the methods of monitoring and mitigation in mountain permafrost regions are facing some challenges in an adaptation to~~ mountain infrastructure, while current mitigation methods struggle to adapt to rapid climate change. This study investigates the Schilthorn site in the Bernese Alps, Switzerland, where the ALT has doubled over the past decade, highlighting its vulnerability to climate change. Using the 1D SNOWPACK model, validated with borehole temperature data, we simulate and assess various passive and active thermal stabilisation strategies (Table 3). These methods aim to cool the ground, regulate seasonal heat exchange, and reduce ALT. One approach establishes a cold thermal barrier powered by collocated solar panels that also shade the surface. After simulating natural site conditions, we test multiple stabilisation systems. Results show that while all methods reduce ground temperatures, combined systems are most effective, with performance depending on the strategy applied.

The simulation results of passive thermal stabilisation with shading of the surface (Section 4.2.1) indicated that this measure alone is not sufficient to create long-term thermal stabilisation of permafrost. It has a good effect during winter, due to natural

cooling; in summer, however, the ALT stays almost unchanged compared to natural conditions (Section 5.2.1). Another passive cooling system consists of a thermal insulation layer on top of the ground (Section 4.2.2). Covering the ground year-round with insulation material does not result in significant thermal stabilisation, while deploying and lifting the insulation layer depending on the season effectively regulate the conductive heat flux near the ground surface, leading to favourable stabilisation effects (Section 5.2.2). The thermal stabilisation seasonal heat flux attenuation method significantly reduces the ALT, although it takes several years to fully achieve this effect.

A pipe system in the ground for active cooling (Section 4.2.3) can create a stable continuous thermal barrier layer but only after a period of 4 years (Section 5.2.3). The best efficiency of a thermal stabilisation system is achieved by combining active and passive methods (Section 5.2.3), which decreases the ALT to only a few tens of centimetres, and results in a stable barrier layer already after the first year simulated. The combination of active cooling, shading, and heat flux attenuation with a temporary thermal insulation layer that reduces warming in summer and favours cooling in winter has the ~~warming processes and require enhancement to adapt to the rapidly changing conditions, and delay further thawing, and increasing of ALT(Haeberli et al., 2023). Our study focuses on a mountain permafrost site Schilthorn in Switzerland, identified as one of the most vulnerable locations, where the ALT has doubled over the past decade (Hauck and Hilbich, 2024).~~ strongest effect (Section 5.3).

We showed the ability of thermal ~~stabilization methods~~ stabilisation methods using renewable energy to delay thawing, protecting exposed infrastructure with adaptable and scalable cooling techniques. This study ~~on mountain permafrost~~ demonstrates that thermal ~~stabilization methods perform just as effectively in mountain permafrost as~~ stabilisation methods applied in alpine permafrost work as effectively as they do in lowland permafrost~~zones (Loktionov et al., 2022)~~. Given their comparable success in different soil types, these methods can be broadly applied to alpine permafrost, extending beyond the specific site studied.

Code and data availability. Data and code used in this study will be published after acceptance of the paper but are available to reviewers upon request.

Appendix A: Natural conditions

A1 Snow height

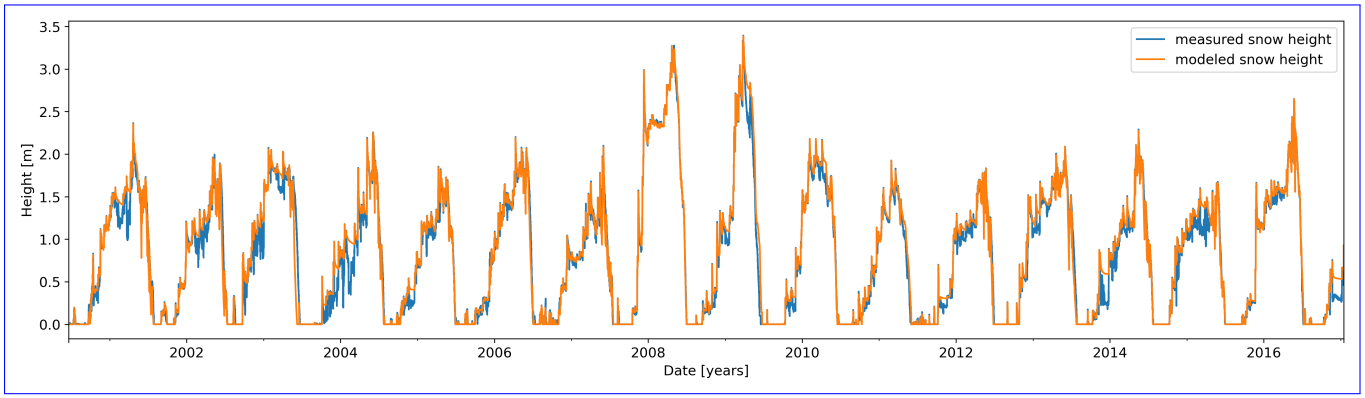

Figure A1. Time series of daily averaged measured and modelled snow height during natural undisturbed conditions at the Schilthorn site from 2000 to 2017.

A2 Ground temperatures

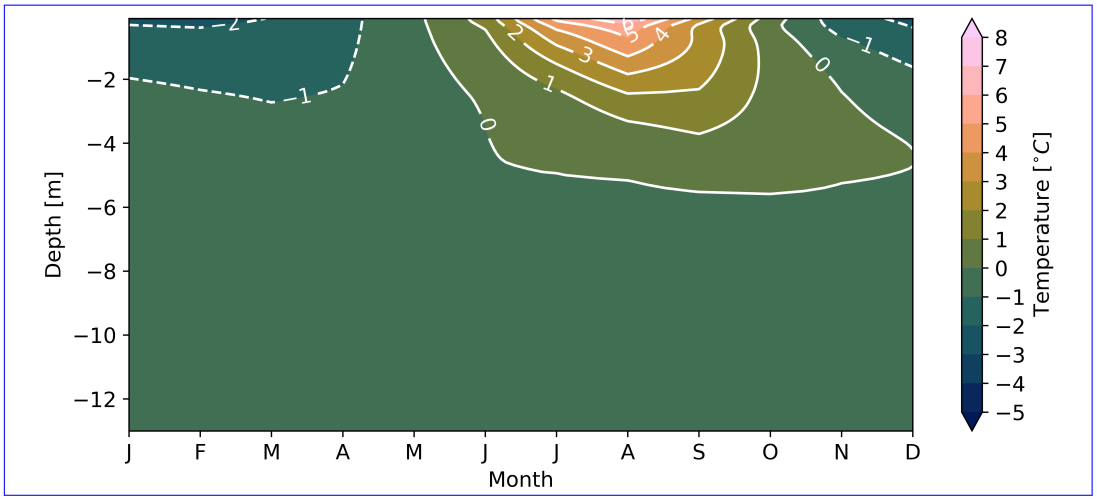

Figure A2. Monthly averaged modelled ground temperatures ~~at the Schilthorn site from 2000 to 2017~~ resulting from natural undisturbed conditions at the Schilthorn site from 2000 to 2017.

Appendix B: Thermal ~~stabilization~~ stabilisation with thermal insulation

B1 Thermal insulation conductive heat flux distribution

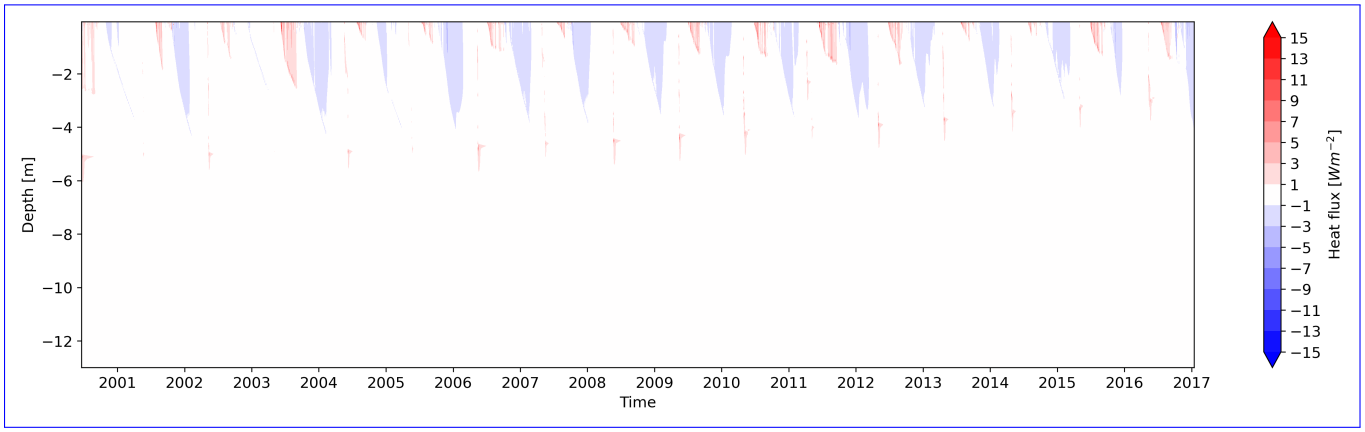

Figure B1. Time series of daily averaged modelled conductive heat flux from thermal insulation experiment using 50 mm thermal insulation layer at the Schilthorn site for the period of 2000 to 2017.

B2 Thermal insulation thickness effect

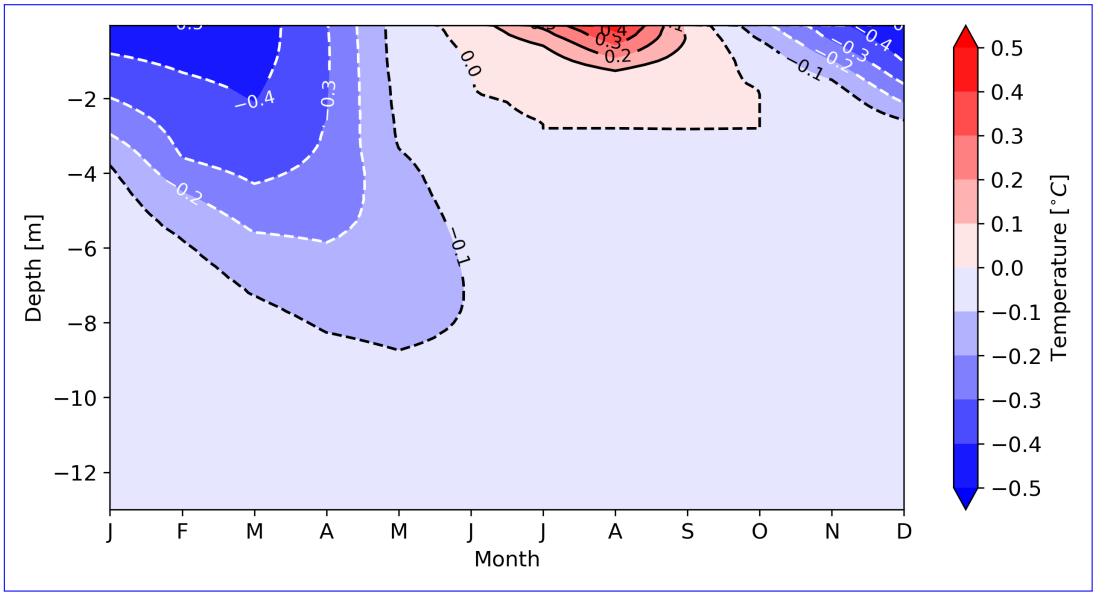

Figure B2. Monthly averaged temperature differences between 50 mm and 100 mm ~~(50 mm - 100 mm)~~ thermal insulation thicknesses.

B3 Heat flux ~~regulation~~ attenuation distribution of conductive heat fluxes

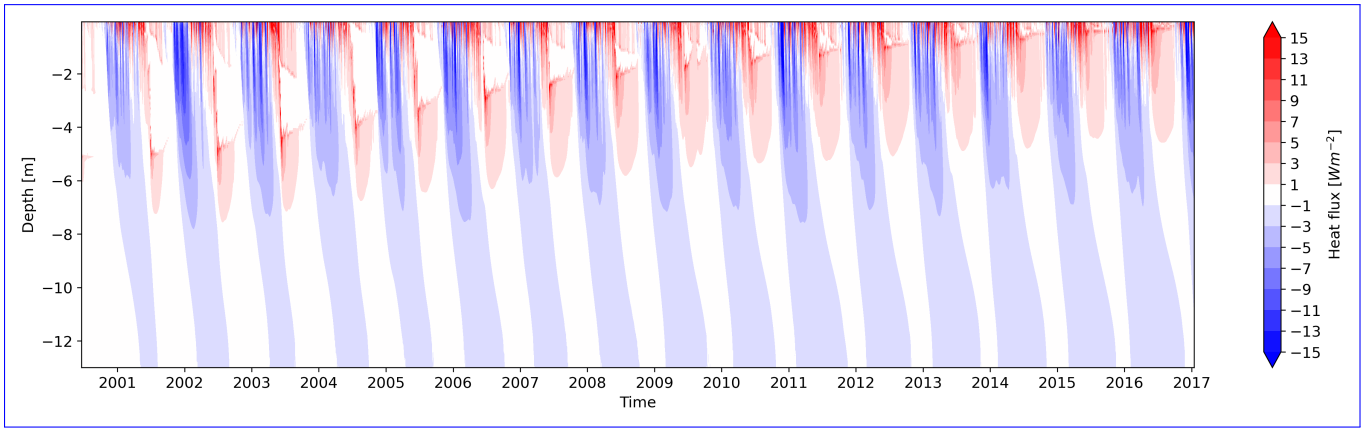

Figure B3. Time series of daily averaged modelled conductive heat flux from the heat transfer ~~regulation~~ attenuation experiment at the Schilthorn site for the period of 2000 to 2017.

Appendix C: Thermal ~~stabilization~~ stabilisation with active cooling

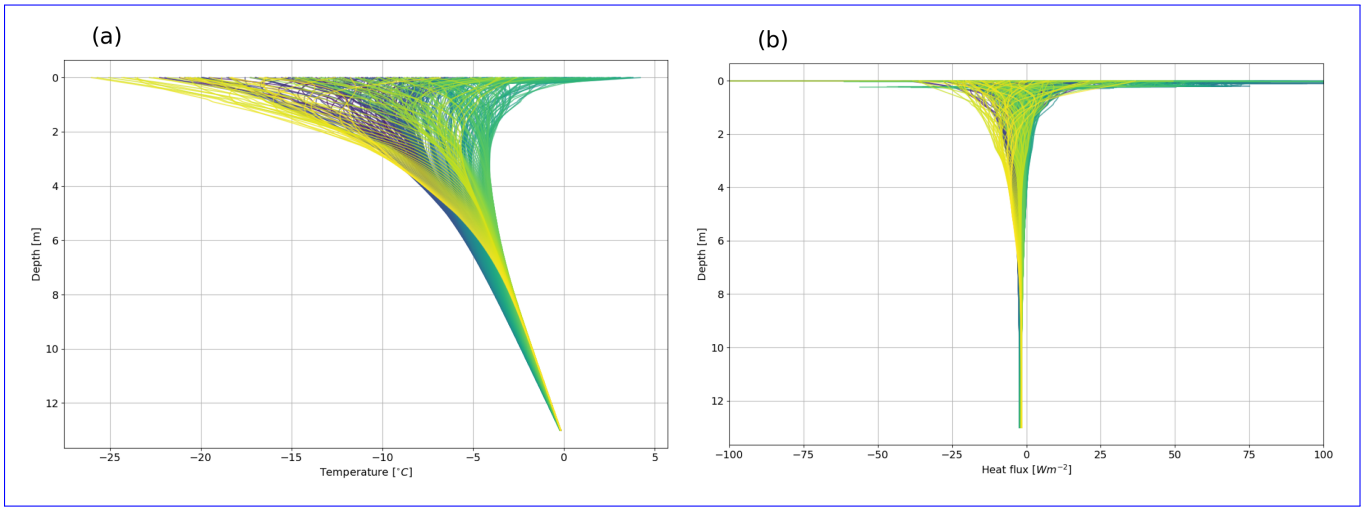

Figure C1. (a) Daily averaged temperature distribution, and (b) daily averaged heat flux distribution for the last year of the simulations, 2016 after 16 years of active cooling and shading.

Appendix D: Thermal stabilisation methods comparison

Table D1. Thermal stabilisation methods comparison.

Experiment number	Model simulation	Max ALT after 16 years, m	Max of monthly averaged ALT over 16 years, m
1	Natural conditions	6.20	5.59
2	Shading of the surface	3.40	2.77
3	Thermal insulation (50 mm) all year round	1.50	2.80
4	Heat flux attenuation	0.26	1.01
5	Active cooling (cooling pipes alone)	0.23	0.12
6	Active and passive cooling (cooling pipes and solar panels)	0.21	0
7	Active and passive cooling (cooling pipes and solar panels) using 50% of energy for cooling	0.92	0.07
8	Active and passive cooling (cooling pipes and solar panels) using 10% of energy for cooling combined with heat flux attenuation	0	0

Author contributions. ES, ML and HH designed the research. ES prepared the data, run the simulations, analysed results and wrote the draft. ML, NW, MP, HH contributed to the results and data analysis and revised the manuscript. ML and HH supervised the research. NW maintained and corrected the SNOWPACK code. MP provided expertise in permafrost processes. All authors contributed to the final version of the manuscript.

Competing interests. The corresponding author has declared that none of the authors have any known competing financial interests or personal relationships that could have influenced the work reported in this paper.

Acknowledgements. We acknowledge MeteoSwiss~~and IMIS~~, IMIS, and PERMOS for providing the observational data used in this research. We ~~acknowledge the editor~~ are grateful to Prof. Hanna Lee~~for~~, the editor, for her valuable feedback and insightful comments, which ~~contributed to the improvement of this~~ greatly improved this manuscript. We appreciate team at the Department of Geosciences, University of Fribourg, for their helpful feedback. We thank Dr. Sergi Gonzàlez Herrero for his suggestions on data presentation and analysis, as well as his valuable recommendations. We acknowledge Egor Yu. Loktionov for his contribution to the development and patenting of the thermal stabilization method employed in this work. We acknowledge the funding support of Swiss Government Excellence Scholarship. Finally, we acknowledge the two anonymous reviewers for their constructive comments and suggestions that enhanced the quality of the manuscript.

References

Alekseev, A., Gribovskii, G., and Vinogradova, S.: Comparison of analytical solution of the semi-infinite problem of soil freezing with numerical solutions in various simulation software, IOP Conference Series: Materials Science and Engineering, 365, 042 059, https://doi.org/10.1088/1757-899X/365/4/042059, 2018.

Asanov, I. M. and Loktionov, E. Y.: Possible benefits from PV modules integration in railroad linear structures, Renewable Energy Focus, 25, 1–3, https://doi.org/10.1016/j.ref.2018.02.003, 2018.

Bavay, M. and Egger, T.: MeteoIO 2.4.2: a preprocessing library for meteorological data, Geoscientific Model Development, 7, 3135–3151, https://doi.org/10.5194/gmd-7-3135-2014, 2014.

BBC News: Arctic Circle oil spill: Russian prosecutors order checks at permafrost sites, https://www.bbc.com/news/world-europe-52941845, accessed on 18 July 2023, 2020.

Biskaborn, B. K., Smith, S. L., Noetzli, J., Matthes, H., Vieira, G., Streletskiy, D. A., Schoeneich, P., Romanovsky, V. E., Lewkowicz, A. G., Abramov, A., Allard, M., Boike, J., Cable, W. L., Christiansen, H. H., Delaloye, R., Diekmann, B., Drozdov, D., Etzelmüller, B., Grosse, G., Guglielmin, M., Ingeman-Nielsen, T., Isaksen, K., Ishikawa, M., Johansson, M., Johannsson, H., Joo, A., Kaverin, D., Kholodov, A., Konstantinov, P., Kröger, T., Lambiel, C., Lanckman, J.-P., Luo, D., Malkova, G., Meiklejohn, I., Moskalenko, N., Oliva, M., Phillips, M., Ramos, M., Sannel, A. B. K., Sergeev, D., Seybold, C., Skryabin, P., Vasiliev, A., Wu, Q., Yoshikawa, K., Zheleznyak, M., and Lantuit, H.: Permafrost is warming at a global scale, Nature Communications, 10, 264, https://doi.org/10.1038/s41467-018-08240-4, number: 1 Publisher: Nature Publishing Group, 2019.

Bommer, C., Phillips, M., and Arenson, L. U.: Practical recommendations for planning, constructing and maintaining infrastructure in mountain permafrost, Permafrost and Periglacial Processes, 21, 97–104, https://doi.org/10.1002/ppp.679, _eprint: https://onlinelibrary.wiley.com/doi/pdf/10.1002/ppp.679, 2010.

Chen, Y., Mandal, J., Li, W., Smith-Washington, A., Tsai, C.-C., Huang, W., Shrestha, S., Yu, N., Han, R. P. S., Cao, A., and Yang, Y.: Colored and paintable bilayer coatings with high solar-infrared reflectance for efficient cooling, Science Advances, 6, eaaz5413, https://doi.org/10.1126/sciadv.aaz5413, publisher: American Association for the Advancement of Science, 2020.

Cheng, G.: A roadbed cooling approach for the construction of Qinghai–Tibet Railway, Cold Regions Science and Technology, 42, 169–176, https://doi.org/10.1016/j.coldregions.2005.01.002, 2005.

Duvillard, P. A., Ravanel, L., Schoeneich, P., Deline, P., Marcer, M., and Magnin, F.: Qualitative risk assessment and strategies for infrastructure on permafrost in the French Alps, Cold Regions Science and Technology, 189, 103 311, https://doi.org/10.1016/j.coldregions.2021.103311, 2021.

Ekici, A., Chadburn, S., Chaudhary, N., Hajdu, L. H., Marmy, A., Peng, S., Boike, J., Burke, E., Friend, A. D., Hauck, C., Krinner, G., Langer, M., Miller, P. A., and Beer, C.: Site-level model intercomparison of high latitude and high altitude soil thermal dynamics in tundra and barren landscapes, The Cryosphere, 9, 1343–1361, https://doi.org/10.5194/tc-9-1343-2015, publisher: Copernicus GmbH, 2015.

Etzelmüller, B., Guglielmin, M., Hauck, C., Hilbich, C., Hoelzle, M., Isaksen, K., Noetzli, J., Oliva, M., and Ramos, M.: Twenty years of European mountain permafrost dynamics—the PACE legacy, Environmental Research Letters, 15, 104 070, https://doi.org/10.1088/1748-9326/abae9d, publisher: IOP Publishing, 2020.

Farinotti, D., Usselmann, S., Huss, M., Bauder, A., and Funk, M.: Runoff evolution in the Swiss Alps: projections for selected high-alpine catchments based on ENSEMBLES scenarios, Hydrological Processes, 26, 1909–1924, https://doi.org/10.1002/hyp.8276, publisher: John Wiley & Sons, Ltd, 2012.

Gruber, S. and Haeberli, W.: Mountain Permafrost, in: Permafrost Soils, edited by Margesin, R., pp. 33–44, Springer, Berlin, Heidelberg, ISBN 978-3-540-69371-0, https://doi.org/10.1007/978-3-540-69371-0_3, 2009.

Grünewald, T., Wolfsperger, F., and Lehning, M.: Snow farming: conserving snow over the summer season, The Cryosphere, 12, 385–400, https://doi.org/10.5194/tc-12-385-2018, 2018.

Haberkorn, A., Wever, N., Hoelzle, M., Phillips, M., Kenner, R., Bavay, M., and Lehning, M.: Distributed snow and rock temperature modelling in steep rock walls using Alpine3D.

Haberkorn, A., Wever, N., Hoelzle, M., Phillips, M., Kenner, R., Bavay, M., and Lehning, M.: Distributed snow and rock temperature modelling in steep rock walls using Alpine3D, The Cryosphere, 11, 585–607, https://doi.org/10.5194/tc-11-585-2017, 2017.

Haeberli, W. and Gruber, S.: Global Warming and Mountain Permafrost, pp. 205–218, Springer Berlin Heidelberg, Berlin, Heidelberg, ISBN 978-3-540-69371-0, https://doi.org/10.1007/978-3-540-69371-0_14, 2009.

Haeberli, W., Noetzli, J., Arenson, L., Delaloye, R., Gärtner-Roer, I., Gruber, S., Isaksen, K., Kneisel, C., Krautblatter, M., and Phillips, M.: Mountain permafrost: development and challenges of a young research field, Journal of Glaciology, 56, 1043–1058, https://doi.org/10.3189/002214311796406121, 2010.

Haeberli, W., Schaub, Y., and Huggel, C.: Increasing risks related to landslides from degrading permafrost into new lakes in de-glaciating mountain ranges, Geomorphology, 293, 405–417, https://doi.org/https://doi.org/10.1016/j.geomorph.2016.02.009, permafrost and periglacial research from coasts to mountains, 2017.

Haeberli, W., Noetzli, J., and Mühll, D. V.: Using Borehole Temperatures for Knowledge Transfer about Mountain Permafrost: The Example of the 35-year Time Series at Murtèl-Corvatsch (Swiss Alps), Journal of Alpine Research | Revue de géographie alpine, https://doi.org/10.4000/rga.11950, number: 111-2 Publisher: Association pour la diffusion de la recherche alpine et UGA Éditions., 2023.

Harris, C., Arenson, L. U., Christiansen, H. H., Etzelmüller, B., Frauenfelder, R., Gruber, S., Haeberli, W., Hauck, C., Hölzle, M., Humlum, O., Isaksen, K., Kääb, A., Kern-Lütschg, M. A., Lehning, M., Matsuoka, N., Murton, J. B., Nötzli, J., Phillips, M., Ross, N., Seppälä, M., Springman, S. M., and Vonder Mühll, D.: Permafrost and climate in Europe: Monitoring and modelling thermal, geomorphological and geotechnical responses, Earth-Science Reviews, 92, 117–171, https://doi.org/https://doi.org/10.1016/j.earscirev.2008.12.002, 2009a.

Harris, C., Arenson, L. U., Christiansen, H. H., Etzelmüller, B., Frauenfelder, R., Gruber, S., Haeberli, W., Hauck, C., Hölzle, M., Humlum, O., Isaksen, K., Kääb, A., Kern-Lütschg, M. A., Lehning, M., Matsuoka, N., Murton, J. B., Nötzli, J., Phillips, M., Ross, N., Seppälä, M., Springman, S. M., and Vonder Mühll, D.: Permafrost and climate in Europe: Monitoring and modelling thermal, geomorphological and geotechnical responses, Earth-Science Reviews, 92, 117–171, https://doi.org/10.1016/j.earscirev.2008.12.002, 2009b.

Hauck, C.: Frozen ground monitoring using DC resistivity tomography, Geophysical Research Letters, 29, 12–1–12–4, https://doi.org/10.1029/2002GL014995, _eprint: https://onlinelibrary.wiley.com/doi/pdf/10.1029/2002GL014995, 2002.

Hauck, C. and Hilbich, C.: Preconditioning of mountain permafrost towards degradation detected by electrical resistivity, Environmental Research Letters, 19, 064 010, https://doi.org/10.1088/1748-9326/ad3c55, publisher: IOP Publishing, 2024.

Hilbich, C.: Time-lapse refraction seismic tomography for the detection of ground ice degradation, The Cryosphere, 4, 243–259, https://doi.org/10.5194/tc-4-243-2010, publisher: Copernicus GmbH, 2010.

Hjort, J., Karjalainen, O., Aalto, J., Westermann, S., Romanovsky, V. E., Nelson, F. E., Etzelmüller, B., and Luoto, M.: Degrading permafrost puts Arctic infrastructure at risk by mid-century, Nature Communications, 9, 5147, https://doi.org/10.1038/s41467-018-07557-4, number: 1 Publisher: Nature Publishing Group, 2018.

Hjort, J., Streletskiy, D., Doré, G., Wu, Q., Bjella, K., and Luoto, M.: Impacts of permafrost degradation on infrastructure, Nature Reviews Earth & Environment, 3, 24–38, https://doi.org/10.1038/s43017-021-00247-8, 2022.

Hoelzle, M., Hauck, C., Mathys, T., Noetzli, J., Pellet, C., and Scherler, M.: Long-term energy balance measurements at three different mountain permafrost sites in the Swiss Alps, Earth System Science Data, 14, 1531–1547, https://doi.org/10.5194/essd-14-1531-2022, publisher: Copernicus GmbH, 2022.

Holtslag, A. a. M. and Bruin, H. A. R. D.: Applied Modeling of the Nighttime Surface Energy Balance over Land, Journal of Applied Meteorology and Climatology, 27, 689–704, https://doi.org/10.1175/1520-0450(1988)027<0689:AMOTNS>2.0.CO;2, publisher: American Meteorological Society Section: Journal of Applied Meteorology and Climatology, 1988.

Hu, T.-f., Liu, J.-k., Hao, Z.-h., and Chang, J.: Design and experimental study of a solar compression refrigeration apparatus (SCRA) for embankment engineering in permafrost regions, Transportation Geotechnics, 22, 100 311, https://doi.org/10.1016/j.trgeo.2019.100311, 2020.

Huss, M., Farinotti, D., Bauder, A., and Funk, M.: Modelling runoff from highly glacierized alpine drainage basins in a changing climate, Hydrological Processes, 22, 3888–3902, https://doi.org/10.1002/hyp.7055, _eprint: https://onlinelibrary.wiley.com/doi/pdf/10.1002/hyp.7055, 2008.

Instanes, A. and Mjureke, D.: Svalbard airport runway. Performance during a climate-warming scenario., Proceedings of the international conferences on the bearing capacity of roads, railways and airfields, https://www.ntnu.no/ojs/index.php/BCRRA/article/view/3224, 2005.

Jansson, P.-E. and Karlberg, L.: Coupled heat and mass transfer model for soil-plant-atmosphere systems. Royal Institute of Technology, Department of Civil and Environmental Engineering, Stockholm, 2004.

Kenner, R.: Permafrost distribution in Switzerland: Ground temperatures and ice content (2018), Zenodo, https://doi.org/10.5281/zenodo.1470165, 2018.

Kenner, R., Noetzli, J., Hoelzle, M., Raetzo, H., and Phillips, M.: Distinguishing ice-rich and ice-poor permafrost to map ground temperatures and ground ice occurrence in the Swiss Alps, The Cryosphere, 13, 1925–1941, https://doi.org/10.5194/tc-13-1925-2019, 2019.

Kenner, R., Noetzli, J., Bazargan, M., and Scherrer, S. C.: Response of alpine ground temperatures to a rising atmospheric 0 °C isotherm in the period 1955–2021, Science of The Total Environment, 924, 171 446, https://doi.org/10.1016/j.scitotenv.2024.171446, 2024.

Lehning, M., Bartelt, P., Brown, B., Russi, T., Stöckli, U., and Zimmerli, M.: snowpack model calculations for avalanche warning based upon a new network of weather and snow stations, Cold Regions Science and Technology, 30, 145–157, https://doi.org/https://doi.org/10.1016/S0165-232X(99)00022-1, 1999a.

Lehning, M., Bartelt, P., Brown, B., Russi, T., Stöckli, U., and Zimmerli, M.: snowpack model calculations for avalanche warning based upon a new network of weather and snow stations, Cold Regions Science and Technology, 30, 145–157, https://doi.org/10.1016/S0165-232X(99)00022-1, 1999b.

Lehning, M., Doorschot, J., and Bartelt, P.: A snowdrift index based on SNOWPACK model calculations, Annals of Glaciology, 31, 382–386, https://doi.org/10.3189/172756400781819770, 2000.

Lehning, M., Bartelt, P., Brown, B., Fierz, C., and Satyawali, P.: A physical SNOWPACK model for the Swiss avalanche warning: Part II. Snow microstructure, Cold Regions Science and Technology, 35, 147–167, https://doi.org/10.1016/S0165-232X(02)00073-3, 2002.

Li, F., Qin, Y., Wu, B., and Wang, T.: Experimental study on the cooling performance of shading boards with different emissivities at the underside, Cold Regions Science and Technology, 169, 102 902, https://doi.org/10.1016/j.coldregions.2019.102902, 2020.

Liu, B. Y. H. and Jordan, R. C.: The interrelationship and characteristic distribution of direct, diffuse and total solar radiation, Solar Energy, 4, 1–19, https://doi.org/10.1016/0038-092X(60)90062-1, 1960.

Loktionov, E., Klokov, A., Tutunin, A., Bakhmadov, A., Sharaborova, E., Sepitko, T., Churkin, S., and Korshunov, A.: Permafrost thermal stabilization using renewable energy sources, Tech. rep., International Permafrost Association (IPA), https://doi.org/10.52381/ICOP2024.152.1, 2024a.

Loktionov, E. Y., Sharaborova, E. S., and Asanov, I. M.: Prospective Sites for Solar-Powered Permafrost Stabilization Systems Integration in Russian Railways, in: 2019 8th International Conference on Renewable Energy Research and Applications (ICRERA), pp. 568–572, https://doi.org/10.1109/ICRERA47325.2019.8996544, iSSN: 2572-6013, 2019.

Loktionov, E. Y., Sharaborova, E. S., and Shepitko, T. V.: A sustainable concept for permafrost thermal stabilization, Sustainable Energy Technologies and Assessments, 52, 102 003, https://doi.org/10.1016/j.seta.2022.102003, 2022.

Loktionov, E. Y., Sharaborova, E. S., Klokov, A. V., Maslakov, A. A., Sotnikova, K. S., and Korshunov, A. A.: Ice cellars preservation technologies to ensure sustainable development of northern settlements, Arctic: Ecology and Economy, 14, 116–126, https://doi.org/10.25283/2223-4594-2024-1-116-126, (In Russian), 2024b.

Luethi, R., Phillips, M., and Lehning, M.: Estimating Non-Conductive Heat Flow Leading to Intra-Permafrost Talik Formation at the Ritigraben Rock Glacier (Western Swiss Alps), Permafrost and Periglacial Processes, 28, 183–194, https://doi.org/10.1002/ppp.1911, _eprint: https://onlinelibrary.wiley.com/doi/pdf/10.1002/ppp.1911, 2017.

Luetschg, M., Lehning, M., and Haeberli, W.: A sensitivity study of factors influencing warm/thin permafrost in the Swiss Alps, Journal of Glaciology, 54, 696–704, https://doi.org/10.3189/002214308786570881, 2008.

Luo, J., Niu, F., Liu, M., Lin, Z., and Yin, G.: Field experimental study on long-term cooling and deformation characteristics of crushed-rock revetment embankment at the Qinghai–Tibet Railway, Applied Thermal Engineering, 139, 256–263, https://doi.org/10.1016/j.applthermaleng.2018.04.138, 2018.

Lütschg, M.: A Model and Field Analysis of the Interaction Between Snow Cover and Alpine Permafrost, Physische Geographie, Geographisches Institut der Universität Zürich, ISBN 9783855432431, https://books.google.ch/books?id=-_37NAAACAAJ, 2005.

Marmy, A., Salzmann, N., Scherler, M., and Hauck, C.: Permafrost model sensitivity to seasonal climatic changes and extreme events in mountainous regions, Environmental Research Letters, 8, 035 048, https://doi.org/10.1088/1748-9326/8/3/035048, publisher: IOP Publishing, 2013.

Marmy, A., Rajczak, J., Delaloye, R., Hilbich, C., Hoelzle, M., Kotlarski, S., Lambiel, C., Noetzli, J., Phillips, M., Salzmann, N., Staub, B., and Hauck, C.: Semi-automated calibration method for modelling of mountain permafrost evolution in Switzerland, The Cryosphere, 10, 2693–2719, https://doi.org/10.5194/tc-10-2693-2016, 2016.

Mergili, M., Jaboyedoff, M., Pullarello, J., and Pudasaini, S. P.: Back calculation of the 2017 Piz Cengalo–Bondo landslide cascade with r.avaflow: what we can do and what we can learn, Natural Hazards and Earth System Sciences, 20, 505–520, https://doi.org/10.5194/nhess-20-505-2020, publisher: Copernicus GmbH, 2020.

Morard, S., Hilbich, C., Mollaret, C., Pellet, C., and Hauck, C.: 20-year permafrost evolution documented through petrophysical joint inversion, thermal and soil moisture data, Environmental Research Letters, 19, 074 074, https://doi.org/10.1088/1748-9326/ad5571, publisher: IOP Publishing, 2024.

Noetzli, J., Hoelzle, M., Haeberli, W., and Al, E.: Mountain permafrost and recent Alpine rock-fall events: a GIS-based approach to determine critical factors, in: Noetzli, J; Hoelzle, M; Haeberli, W (2003). Mountain permafrost and recent Alpine rock-fall events: a GIS-based approach to determine critical factors. In: Phillips, M; et al. Permafrost: proceedings of the eighth International Conference on Permafrost. Lisse, The Netherlands: Balkema Publishers, 827-832., edited by Phillips, M., pp. 827–832, Balkema Publishers, Lisse, The Netherlands, ISBN 978-90-5809-585-5, https://doi.org/10.5167/uzh-33321, issue: 2 Number: 2, 2003.

Noetzli, J., Isaksen, K., Barnett, J., Christiansen, H. H., Delaloye, R., Etzelmüller, B., Farinotti, D., Gallemann, T., Guglielmin, M., Hauck, C., Hilbich, C., Hoelzle, M., Lambiel, C., Magnin, F., Oliva, M., Paro, L., Pogliotti, P., Riedl, C., Schoeneich, P., Valt, M., Vieli, A., and Phillips, M.: Enhanced warming of European mountain permafrost in the early 21st century, Nature Communications, 15, 10 508, https://doi.org/10.1038/s41467-024-54831-9, publisher: Nature Publishing Group, 2024.

Olefs, M. and Lehning, M.: Textile protection of snow and ice: Measured and simulated effects on the energy and mass balance, Cold Regions Science and Technology, 62, 126–141, https://doi.org/10.1016/j.coldregions.2010.03.011, 2010.

Olson, M. and Rupper, S.: Impacts of topographic shading on direct solar radiation for valley glaciers in complex topography, The Cryosphere, 13, 29–40, https://doi.org/10.5194/tc-13-29-2019, publisher: Copernicus GmbH, 2019.

Pellet, C., Hilbich, C., Marmy, A., and Hauck, C.: Soil Moisture Data for the Validation of Permafrost Models Using Direct and Indirect Measurement Approaches at Three Alpine Sites, Frontiers in Earth Science, 3, https://doi.org/10.3389/feart.2015.00091, 2016.

Phillips, M., Ladner, F., Müller, M., Sambeth, U., Sorg, J., and Teysseire, P.: Monitoring and reconstruction of a chair-lift midway station in creeping permafrost terrain, Grächen, Swiss Alps, Cold Regions Science and Technology, 47, 32–42, https://doi.org/10.1016/j.coldregions.2006.08.014, 2007.

Pruessner, L., Phillips, M., Farinotti, D., Hoelzle, M., and Lehning, M.: Near-surface ventilation as a key for modeling the thermal regime of coarse blocky rock glaciers, Permafrost and Periglacial Processes, 29, 152–163, https://doi.org/10.1002/ppp.1978, _eprint: https://onlinelibrary.wiley.com/doi/pdf/10.1002/ppp.1978, 2018.

Pruessner, L., Huss, M., Phillips, M., and Farinotti, D.: A Framework for Modeling Rock Glaciers and Permafrost at the Basin-Scale in High Alpine Catchments, Journal of Advances in Modeling Earth Systems, 13, https://doi.org/10.1029/2020MS002361, 2021.

Qin, Y., Li, Y., and Bao, T.: An experimental study of reflective shading devices for cooling roadbeds in permafrost regions, Solar Energy, 205, 135–141, https://doi.org/10.1016/j.solener.2020.05.054, 2020.

Qiu, T., Wang, G., Xu, Q., and Ni, G.: Study on the thermal performance and design method of solar reflective–thermal insulation hybrid system for wall and roof in Shanghai, Solar Energy, 171, 851–862, https://doi.org/10.1016/j.solener.2018.07.036, 2018.

Quinton, W., Hayashi, M., and Chasmer, L.: Permafrost-thaw-induced land-cover change in the Canadian subarctic: implications for water resources, Hydrological Processes, 25, 152–158, https://doi.org/10.1002/hyp.7894, _eprint: https://onlinelibrary.wiley.com/doi/pdf/10.1002/hyp.7894, 2011.

Ramamurthy, P., Sun, T., Rule, K., and Bou-Zeid, E.: The joint influence of albedo and insulation on roof performance: A modeling study, Energy and Buildings, 102, 317–327, https://doi.org/10.1016/j.enbuild.2015.06.005, 2015.

Schaefer, K., Lantuit, H., Romanovsky, V. E., Schuur, E. A. G., and Witt, R.: The impact of the permafrost carbon feedback on global climate, Environmental Research Letters, 9, 085 003, https://doi.org/10.1088/1748-9326/9/8/085003, publisher: IOP Publishing, 2014.

Scherler, M., Hauck, C., Hoelzle, M., Stähli, M., and Völksch, I.: Meltwater infiltration into the frozen active layer at an alpine permafrost site, Permafrost and Periglacial Processes, pp. 325–334, https://doi.org/10.1002/ppp.694, 2010.

Schlögl, S., Lehning, M., Nishimura, K., Huwald, H., Cullen, N. J., and Mott, R.: How do Stability Corrections Perform in the Stable Boundary Layer Over Snow?, Boundary-Layer Meteorology, 165, 161–180, https://doi.org/10.1007/s10546-017-0262-1, 2017.

Schmucki, E., Marty, C., Fierz, C., and Lehning, M.: Evaluation of modelled snow depth and snow water equivalent at three contrasting sites in Switzerland using SNOWPACK simulations driven by different meteorological data input, Cold Regions Science and Technology, 99, 27–37, https://doi.org/10.1016/j.coldregions.2013.12.004, 2014.

Sharaborova, E., Loktionov, E., and Shepitko, T.: Method for thermally stabilizing permafrost soils, patent WO/2022/075889, WIPO, 2022a.

Sharaborova, E. S. and Loktionov, E. Y.: SOIL THERMAL STABILIZATION METHOD DUE TO YEAR-ROUND REGULATION OF HEAT TRANSFER, patent RU 2 779 706 C1, 2022.

Sharaborova, E. S., Shepitko, T. V., and Loktionov, E. Y.: Experimental Proof of a Solar-Powered Heat Pump System for Soil Thermal Stabilization, Energies, 15, 2118, https://doi.org/10.3390/en15062118, number: 6 Publisher: Multidisciplinary Digital Publishing Institute, 2022b.

Smith, S. L., O'Neill, H. B., Isaksen, K., Noetzli, J., and Romanovsky, V. E.: The changing thermal state of permafrost, Nature Reviews Earth & Environment, 3, 10–23, https://doi.org/10.1038/s43017-021-00240-1, number: 1 Publisher: Nature Publishing Group, 2022.

Solargis: Global Horizontal Irradiation Switzerland, The World Bank, Source: Global Solar Atlas 2.0, Solar resource data: Solargis, https://solargis.com/maps-and-gis-data/download/switzerland, 2020.

Strand, S. M., Christiansen, H. H., Johansson, M., Åkerman, J., and Humlum, O.: Active layer thickening and controls on interannual variability in the Nordic Arctic compared to the circum-Arctic, Permafrost and Periglacial Processes, 32, 47–58, https://doi.org/https://doi.org/10.1002/ppp.2088, 2021.

Swiss Permafrost Monitoring Network (PERMOS): Swiss Permafrost Monitoring Network Database (PERMOS Database), https://doi.org/10.13093/permos-2024-01, data format: ASCII text, zipped; Data size: 38 MB; Spatial coverage: Swiss Alps, Lat (45.9,46.8), Lon (6.8,10.0); Temporal coverage: 1987 to 2023-09-30; Instruments: thermistor chains, miniature temperature loggers, electrical resistivity tomography, dGPS, total station, 2024.

Swiss Permafrost Monitoring Network (PERMOS) and Hoelzle, M.: Energy balance measurements at three PERMOS sites: Corvatsch, Schilthorn, Stockhorn, https://doi.org/10.13093/permos-meteo-2021-01, 2021.

Tian, Y., Yang, Z., Liu, Y., Cai, X., and Shen, Y.: Long-term thermal stability and settlement of heat pipe-protected highway embankment in warm permafrost regions, Engineering Geology, 292, 106 269, https://doi.org/https://doi.org/10.1016/j.enggeo.2021.106269, 2021.

Wagner, F. M., Mollaret, C., Günther, T., Kemna, A., and Hauck, C.: Quantitative imaging of water, ice and air in permafrost systems through petrophysical joint inversion of seismic refraction and electrical resistivity data, Geophysical Journal International, 219, 1866–1875, https://doi.org/10.1093/gji/ggz402, 2019.

Walter, F., Amann, F., Kos, A., Kenner, R., Phillips, M., de Preux, A., Huss, M., Tognacca, C., Clinton, J., Diehl, T., and Bonanomi, Y.: Direct observations of a three million cubic meter rock-slope collapse with almost immediate initiation of ensuing debris flows, Geomorphology, 351, 106 933, https://doi.org/10.1016/j.geomorph.2019.106933, 2020.

Wang, P., Huang, Q., Tang, Q., Chen, X., Yu, J., Pozdniakov, S. P., and Wang, T.: Increasing annual and extreme precipitation in permafrost-dominated Siberia during 1959–2018, Journal of Hydrology, 603, 126 865, https://doi.org/10.1016/j.jhydrol.2021.126865, 2021.

Wang, Z., Kim, Y., Seo, H., Um, M.-J., and Mao, J.: Permafrost response to vegetation greenness variation in the Arctic tundra through positive feedback in surface air temperature and snow cover, Environmental Research Letters, 14, 044 024, https://doi.org/10.1088/1748-9326/ab0839, publisher: IOP Publishing, 2019.

Weber, S., Beutel, J., Faillettaz, J., Hasler, A., Krautblatter, M., and Vieli, A.: Quantifying irreversible movement in steep, fractured bedrock permafrost on Matterhorn (CH), The Cryosphere, 11, 567–583, https://doi.org/10.5194/tc-11-567-2017, 2017.

Westermann, S., Ingeman-Nielsen, T., Scheer, J., Aalstad, K., Aga, J., Chaudhary, N., Etzelmüller, B., Filhol, S., Kääb, A., Renette, C., Schmidt, L. S., Schuler, T. V., Zweigel, R. B., Martin, L., Morard, S., Ben-Asher, M., Angelopoulos, M., Boike, J., Groenke, B., Miesner, F., Nitzbon, J., Overduin, P., Stuenzi, S. M., and Langer, M.: The CryoGrid community model (version 1.0) – a multi-physics toolbox for climate-driven simulations in the terrestrial cryosphere, Geoscientific Model Development, 16, 2607–2647, https://doi.org/10.5194/gmd-16-2607-2023, publisher: Copernicus GmbH, 2023.

Wever, N., Fierz, C., Mitterer, C., Hirashima, H., and Lehning, M.: Solving Richards Equation for snow improves snowpack meltwater runoff estimations in detailed multi-layer snowpack model, The Cryosphere, 8, 257–274, https://doi.org/10.5194/tc-8-257-2014, 2014.

Wever, N., Schmid, L., Heilig, A., Eisen, O., Fierz, C., and Lehning, M.: Verification of the multi-layer SNOWPACK model with different water transport schemes, The Cryosphere, 9, 2271–2293, https://doi.org/10.5194/tc-9-2271-2015, 2015.

Yinfei, D., Shengyue, W., Shuangjie, W., and Jianbing, C.: Cooling permafrost embankment by enhancing oriented heat conduction in asphalt pavement, Applied Thermal Engineering, 103, 305–313, https://doi.org/10.1016/j.applthermaleng.2016.04.115, 2016.

Zappone, A. and Kissling, E.: SAPHYR: Swiss Atlas of Physical Properties of Rocks: the continental crust in a database, Swiss Journal of Geosciences, 114, 13, https://doi.org/10.1186/s00015-021-00389-3, 2021.

Zhang, M., Pei, W., Lai, Y., Niu, F., and Li, S.: Numerical study of the thermal characteristics of a shallow tunnel section with a two-phase closed thermosyphon group in a permafrost region under climate warming, International Journal of Heat and Mass Transfer, 104, 952–963, https://doi.org/10.1016/j.ijheatmasstransfer.2016.09.010, 2017.

Zhao, Y. and Yang, Z. J.: Historical and long-term climate trends in warm permafrost regions: A case study of Bethel, AK, Cold Regions Science and Technology, 204, 103 677, https://doi.org/10.1016/j.coldregions.2022.103677, 2022.

Zhu, X., Wu, T., Li, R., Xie, C., Hu, G., Qin, Y., Wang, W., Hao, J., Yang, S., Ni, J., and Yang, C.: Impacts of Summer Extreme Precipitation Events on the Hydrothermal Dynamics of the Active Layer in the Tanggula Permafrost Region on the Qinghai-Tibetan Plateau, Journal of Geophysical Research: Atmospheres, 122, 11,549–11,567, https://doi.org/10.1002/2017JD026736, _eprint: https://onlinelibrary.wiley.com/doi/pdf/10.1002/2017JD026736, 2017.